МІНІСТЕРСТВО ОСВІТИ І НАУКИ, МОЛОДІ ТА СПОРТУ УКРАЇНИ
НАЦІОНАЛЬНИЙ ТЕХНІЧНИЙ УНІВЕРСИТЕТ УКРАЇНИ “КИЇВСЬКИЙ ПОЛІТЕХНІЧНИЙ ІНСТИТУТ”

Механіко-машинобудівний інститут
(назва факультету, інституту)

Динаміки і міцності машин та опору матеріалів
(назва кафедри)

"На правах рукопису"
УДК__________

«До захисту допущено»
Завідувач кафедри
_____________Піскунов С.О.
(підпис) (ініціали, прізвище)

“___”_____________20___р.

МАГІСТЕРСЬКА ДИСЕРТАЦІЯ

зі спеціальності _131 Прикладна механіка____________________________
(код та назва спеціальності)

на тему: Проектування високонавантаженого двозрізного з'єднання метал-композит мінімальної маси

Студент групи МП-83мп Житнік Тетяни Олегівни __________
(підпис) (шифр групи) (прізвище, ім’я, по батькові)

Науковий керівник к. т. н., доцент Онищенко Є. Є. _________

(вчені ступінь та звання, прізвище, ініціали)

Рецензент
д.т.н. професор __ _________ Данильченко Ю.М.
(посада, науковий ступінь, вчене звання) (підпис) (ініціали, призвище)

Київ 2019

Abstract

The master`s degree dissertation for the amount of work is 60 pages, 36 figures, 11 tables and contains 27 literatures.

The object of the work is double shear composite- metal joint.

The main goal of this dissertation is rational weight reduction of the compound.

The design is done using semi-empirical methods. All calculations are carried out in Excel. Since the calculation is carried out according to a foreign method, all calculations are performed in the American measurement system.

As a result of this work is the creation of a universal template of calculation double-shear joint. Universality lies in the fact that existing programs are complex and not easy to use, or expensive value. This program can be used on any computer.

It was also designed double-cut metal-composite compound of minimum mass - which was the purpose of this dissertation

Реферат

Дисертація на здобуття наукового ступеня магістра, обсяг роботи складає 60 сторінок, 36 рисунків, 11 таблиць і містить 27 літературних джерел.
Об'єктом даної дисертації є високонавантажене двозрізне з'єднання метал-композит.
Головною метою цієї дисертації є раціональне зменшення маси з'єднання.
Дизайн робиться за допомогою напівемпіричних методів. Всі розрахунки проводяться в Excel. Оскільки розрахунок проводиться за іноземним методом, всі обчислення проводяться в американській системі вимірювань

Contents

INTRODUCTION

Composite material is made by combining two or more materials – often ones that have very different properties. The two materials work together to give the composite unique properties. However, within the composite you can easily tell the different materials apart as they do not dissolve or blend into each other.

Aluminum - is a material that has a low weight and toughness. It can be cast, worked, machine-operated and welded with ease. Aluminum is not indicated for high-temperature areas. Due to its lightweight properties, it is indicated for use in aircraft and food cans as well as pistons, cars, railways and kitchen tools.

Steel - is produced by incorporating iron molecules to carbon to make it tougher. Alloy Steel is even more hard and dense as it also includes the addition of heavy metals like chromium and nickel. Steel is basically produced by warming and melting iron in direct fire heaters and then transferred into molds to shape steel bars. Steel is very common in the building and manufacturing fields.

Titanium is a strong, light metal. It is as strong as steel and twice as strong as aluminum, but is 45% lighter than steel and only 60% heavier than aluminum. Titanium is not easily corroded by sea water and is used in propeller shafts, rigging and other parts of boats that are exposed to sea water. Titanium and titanium alloys are used in airplanes, missiles and rockets where strength, low weight and resistance to high temperatures are important. Since titanium does not react within the human body, it is used to create artificial hips, pins for setting bones and for other biological implants. Unfortunately, the high cost of titanium has limited its widespread use

Metal-Composite structures have a wide array of applications, most notably in the automotive, marine, and aerospace disciplines. The joining mechanism between the material constituents is arguably the most critical component of any structure. Mechanical fasteners used in riveted and bolted joints are prevalent in metallic aircraft structures, where they offer a rapid and convenient method of assembling large structures from smaller components. The load-bearing mechanisms of metallic joints are well understood and easily predicted. The use of mechanical fasters in composite structures is also allowed, but this comes with significant strength and fatigue penalties. Nonetheless, mechanical fasteners are still widely used in the construction of composite and/or hybrid structures, especially when load transfer has to be achieved between composite and metallic components.

Bonding composites to metals:

- Titanium (preferred)
- Steel (acceptable)
- Aluminum (not recommended) – Composite to aluminum (corrosion resistant aluminum) splice joint may be used under special circumstances.

Titanium (Ti) alloy and advanced composites are two important materials with high specific strength and stiffness and have been widely used to manufacture the majority of light-weight structural parts of novel aerospace vehicles [1]. Titanium has found significant use in contact with polymeric composite components because titanium is more galvanically compatible with carbon fibers than aluminum and has a relatively good match of thermal expansion coefficients. Mechanical fastening and adhesive bonding are conventional methods for joining and repairing metal and/or composite parts [2]

1. OVERVIEW OF EXISTING DESIGN OF HIGHLY LOADED METAL-COMPOSITE JOINTS

The joining of metal structures is an established technology that involves riveting, bolting, welding, adhesives, brazing, soldering and other methods. By contrast, the technology of joining composites is less well developed, but no less important [3]. To avoid offsetting the weight gain that is realised from using composite structures, it is important that an efficient joint design is used. Conventional processes for metal to composite joining, as listed by Tierney et al. [3] included mechanical fastening and adhesive bonding. A review by Stokes [4] also includes mechanical fastening and bonding. Stokes [4], however went further to reclassify bonding process to include adhesive bonding, solvent bonding and welding. Vicík et al. [5] listed three options namely; mechanical fastening, adhesive bonding and rivet-bonding. However, Moroni et al. [6], have included a new class of metal to composite joint, namely hybrid joining. This class involves the combined use of mechanical fastening together with bonding. From the literature, one can therefore conclude that there are three basic means of joining metal to composites (1) Mechanical joining (2) Adhesive joining and (3) hybrid joining processes.

1.1 Mechanical Joining

Mechanical fastening refers to the use of bolts and rivets to bond composites to other metals. Mechanical fasteners are mainly used for single lap joints (rivets and bolts), double lap joints (bolts), and for flanges (bolts) [3]. The high tensile strength and peel force of bolts and rivets, tolerance to thermal and high humidity environments, simplicity of use and ease of repair, make this joining technique most popular [3;7]. However, damage to the reinforcing fibres and weakening of the cross-section through drilling, stress concentrations around the bearing holes and problems with fitting clearance, are major drawbacks for this technique, especially when applied to CFRP [7 and 8]. In addition, the fasteners themselves and joint overlap are an important source of weight increase [3].

Net tension failure is influenced by the tensile strength of the fibers at fastened joints, witch is maximized when the fastener spacing is approximately four times the fastener diameter (see Fig 1.2). Smaller spacing result in the cutting of too many fibers, while larger spacing result in bearing failures, in which the material is compressed by excessive pressure caused by a small bearing area:

- Use minimum fastener spacing as show in Fig 1.1
- Pad up to reduce net section stress [26]

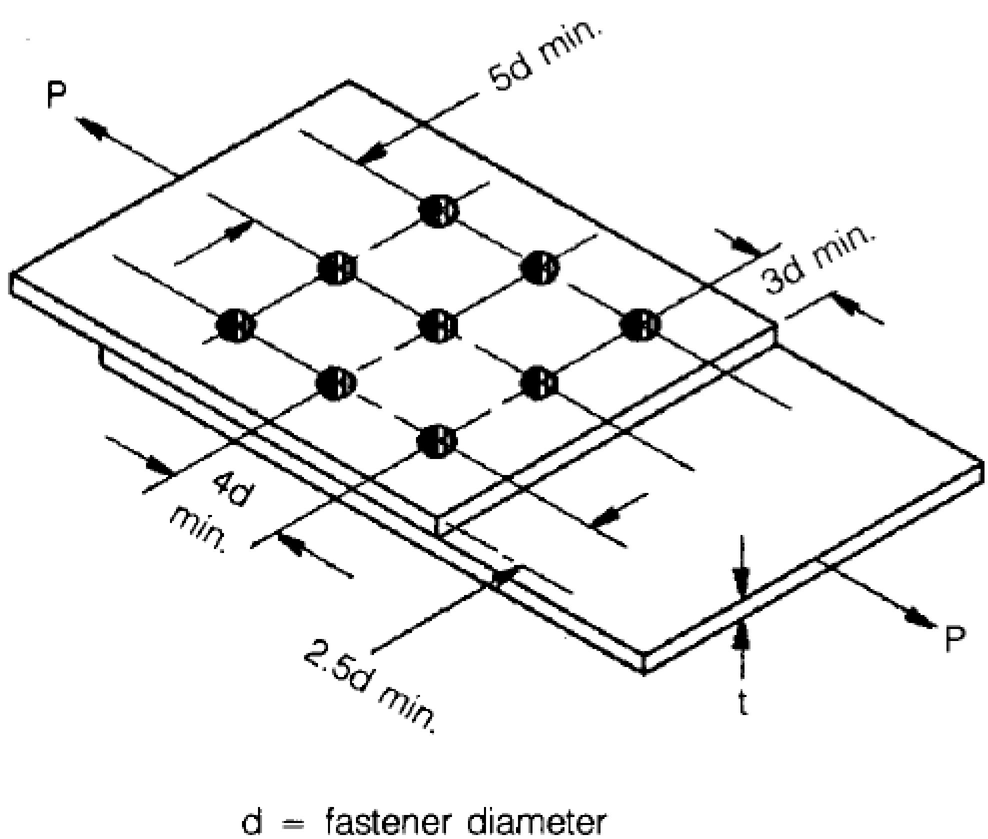

Fig 1.1 Minimum Fastener spacing and Edge Distance

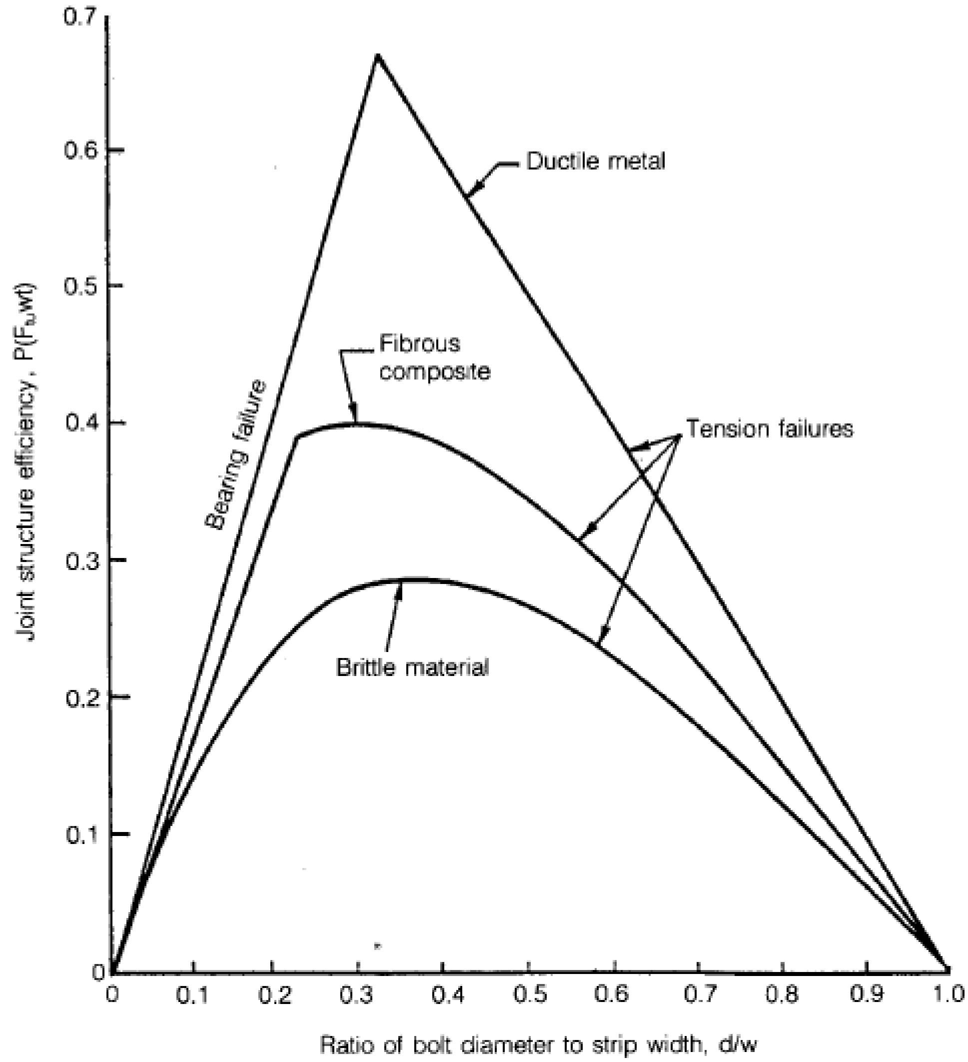

Fig 1.2 Relation Between Strengh of Fastened Joints in Ductile , Brittle, and Composite Materials

1.2 Adhesive Joining

Adhesive joining involves the use of adhesives which hold materials together by surface attachment [3]. Adhesives are normally epoxy resin based, but can be acrylic, phenolic, or polyurethane based. They come in liquid, paste or film form and cure at temperatures from room temperature to 170°C. Adhesively bonded joints have many advantages, such as light weight, a uniform stress distribution, design flexibility, simplicity of fabrication and the ability to bond structural components with different mechanical and thermal properties. Nevertheless, adhesive bonded joints cannot be disassembled without damage. Furthermore, these joints are very sensitive to environmental factors like humidity and temperature, in addition to other design parameters, such as bonding clearances, type and structure of adherend and surface roughness and can have low toughness and creep resistance. The most serious problem for adhesive bonding, however, is the uncertainty regarding the long-term structural integrity due to environmental degradation. This failure behaviour can result in the introduction of "safety-rivets", or an increased overlap of the joining partners, which again increases weight [1; 3; 7; 9; 11; 12].

1.3 Hybrid Joining and Hyper-Joints

The concept of combining different joining technologies and materials is referred to as hybrid joining [1] In hybrid joining two or more operations are carried out either simultaneously, or sequentially, leading to enhanced properties of the joint due to synergetic load bearing interaction under service conditions [10; 7; and 1]. Studies on hybrid joining have shown such techniques offer improved mechanical properties. For example, Kolesnikov et al. [10] have increased joint-strengths in their research through the implantation of titanium-metal-foils in a CFRP layup. Likewise, [12.] was able to delay failure and improve the energy absorbed in the process by the use of pins that were created on the surface of the metal substrate. Similarly, [7] have investigated a hybrid mechanical fastened and bonded joints and found that the combination of the two joining methods induced a more progressive failure propagation, with increased joint strength, than would have been possible using each method Rotimi Joseph Oluleke - Metallurgical Performance of Hyper-Joint Pins in Composite to Metal Joining - 2014 Page 44 individually. Similar results have been observed by Lee et al. and by other noted researchers [6; 13; 14; 15]. Thus, combining adhesive bonding with mechanical joining can offer advantages in terms of load bearing capacity when high levels of both static and dynamic mechanical resistance are required in composite to metal joints. This principle is the basis for this current project.

The Hyper– Joints studied in this project were an innovative form of hybrid joints with the same intent of combining the benefits of mechanical joining with adhesive bonding. Like other hybrid joining processes, the goal with hyper-joints is the formation of an integral joint between the composite material and the metal component to form a composite structure having excellent load bearing capacity. Hyper-joints involve the use of arrays of small metal pins/protrusion which are manufactured on to the surface of the base metal. The metal pins/protrusions are then integrated with the composite laminate without breaking the fibres before curing the resin. This improves the joint strength both via the adhesion and mechanical fit through the thickness of the composite, as shown in figure 2.3 [12]. The small size of the pins (not more than 3 mm but more typically ~ 1 mm in diameter) and the means of providing the mechanical joining clearly distinguish this novel approach from conventional hybrid joining process. The pins must be small in diameter to avoid damaging the composite on insertion. The small size and geometry of the pins thus limits the manufacturing routes that can be used. Within this review, three methods; AM, Surfi-Sculpt and APW, which can be used to manufacture these types of hyper joint pin arrays, will be considered.

2. OVERWIEW OF METHODS FOR CALCULATING HIGHLY LOADED METAL-COMPOSITE JOINS

The fastener flexibility concept was introduced by Tate & Rosenfelt in 1946 [23], under the alias `bolt constant', due to a desire to calculate load distribution in joints with multiple rows. It is defined by assuming a linear relationship between the displacement due to the presence of the fastener, and the load transfer. The fastener flexibility f can be written as

$$f = \frac{1}{k} = \frac{\delta}{P_{LT}} \tag{2.1}$$

where k is the fastener stiffness, P_{LT} the load transferred by the fastener (defined in Figure 2.1), and δ the contribution to the total displacement of the joint disregarding the elongation PL/EA of the plates. Thus, the fastener flexibility includes all phenomena that affect the flexibility of the joint (apart from plate flexibility) such as fastener deformation, fastener tilt, and deformation of fastener holes. In determining the fastener flexibility experimentally, there are several approaches, of which a few are described here.

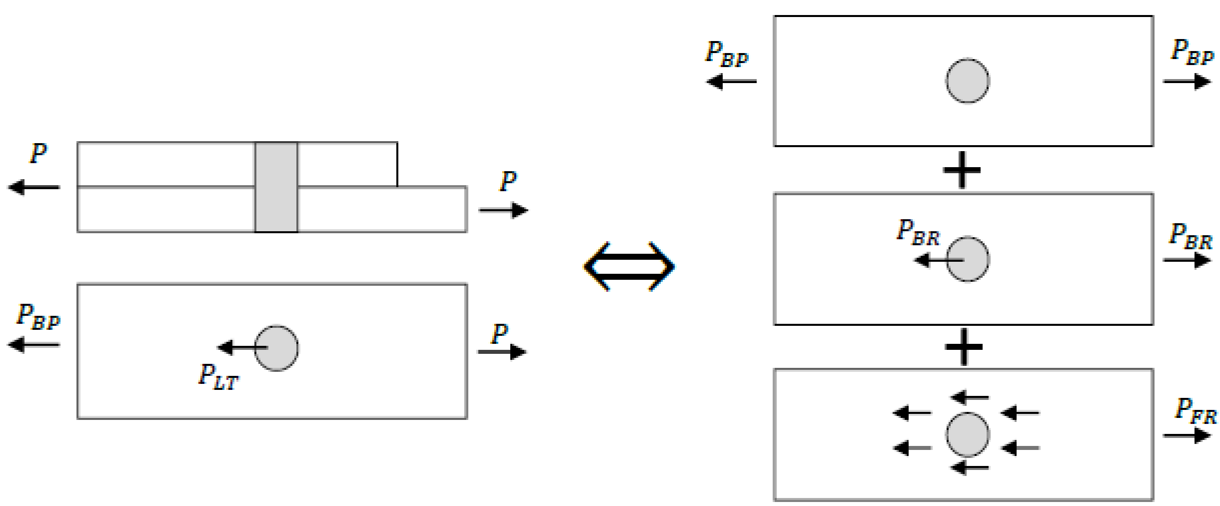

Fig. 2.1 Forces acting on a joint: transferred load *(P_{LT})*, bypassing force *(P_{BP})*, bearing force *(P_{BR})*, frictional force *(P_{FR})*

Jarfall [24] measured the gap *g* of Figure 2.2 for the applied force *2P*.

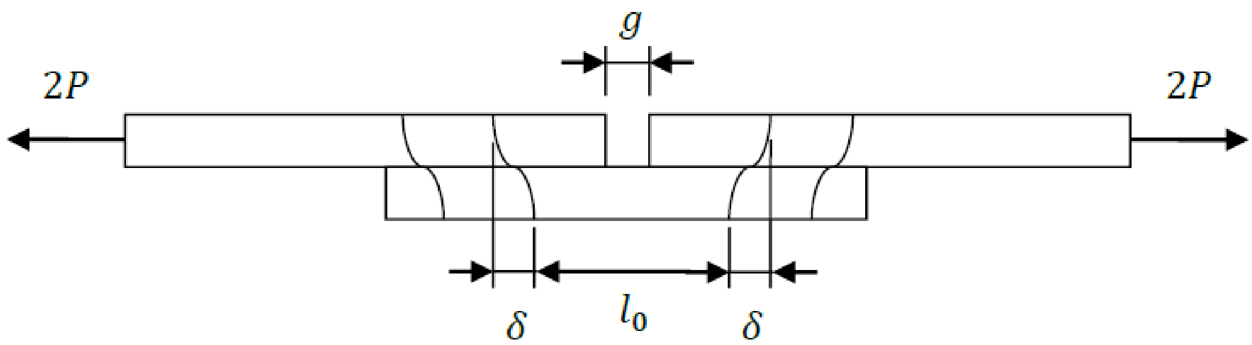

Fig 2.2: Finding fastener flexibility (Jarfall)

The gap *g* relates to δ as

$$\Delta g = \Delta l_0 + 2\delta \tag{2.2}$$

This yields

$$\frac{\partial g}{\partial P} = \frac{2l_0}{AE} + 2f \tag{2.3}$$

and the fastener flexibility becomes

$$f = \frac{1}{2}\frac{\partial g}{\partial P} - \frac{l_0}{AE} \tag{2.4}$$

For the double shear geometry in Figure 2.3, Huth [26] obtained the fastener flexibility by measuring the total displacement between points *A* and *B*, which is written as

$$\Delta l_{tot} = \delta + \Delta l_1 + \Delta l_2 \tag{2.5}$$

From this, δ becomes

$$\delta = \Delta l_{tot} - (\Delta l_1 + \Delta l_2) = \Delta l_{tot} - \Delta l_{elast} \tag{2.6}$$

Where

$$\Delta l_{elast} = \frac{P}{\omega}\left(\frac{l_1}{t_1 E_1} + \frac{l_2}{t_2 E_2}\right) \tag{2.7}$$

The fastener flexibility is then found as

$$f = \frac{\delta}{P} \tag{2.8}$$

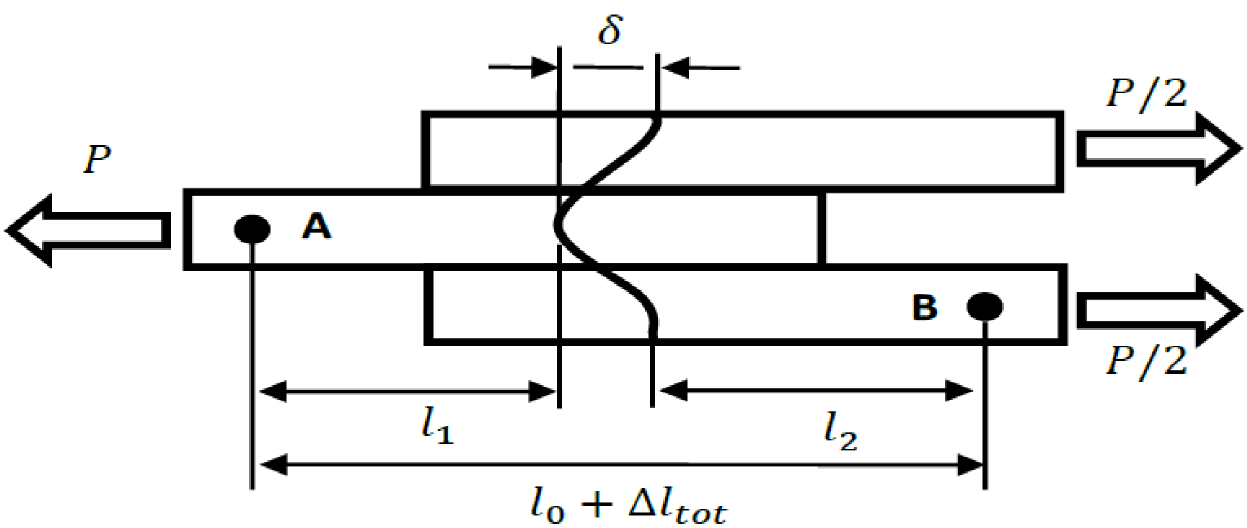

Fig 2.3: Finding fastener flexibility (Huth, double shear)

The relationship between force and displacement is in reality non-linear, and therefore there are several ways to identify a fastener flexibility (as a constant) from experimental data. Jarfall [24] describes some of these methods thoroughly. The way that is probably most representative when striving for an elastic model to describe the behavior of a joint, is the Jarfall alternative *d*, which was also used by Huth. Figure 2.4 shows a sketch of the characteristic behavior of a joint when subjected to cyclically increasing load, where also the fastener flexibility as obtained by Huth is indicated.

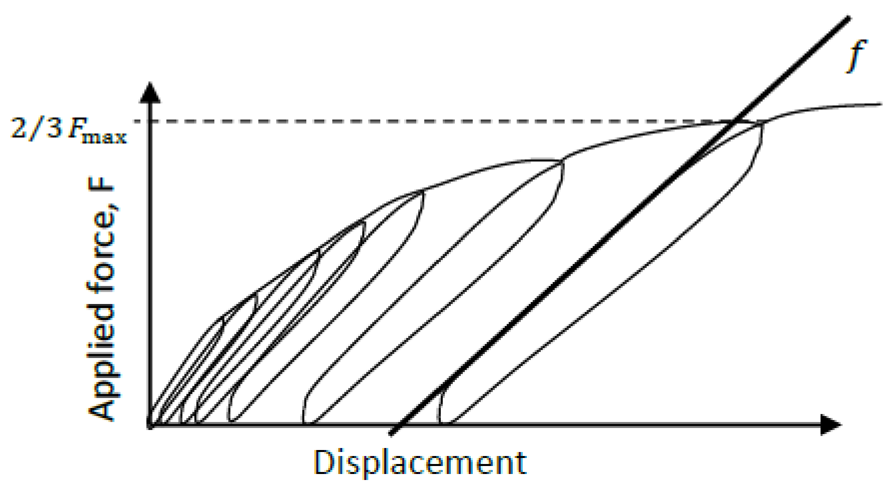

Fig 2.4: Example of measured fastener flexibility

As seen, there are several ways to find the fastener flexibility of Eq. experimentally. Many have attempted - via testing on geometries with varying parameters - to create methods for describing the joint behavior by calculating the fastener flexibility as a function of these parameters. These include empirical formulas derived from specific types of joints and materials by Grumman, Huth , Boeing , Douglas , Tate & Rosenfeld and others, using an analytical approach such as methods by Barrois and ESDU. The great variety of available methods is due to the fact that they have been derived using diferent simplifications and/or thatthey apply to specific materials or specific types of joints.

Things that affect the joint behavior include bolt pre-tension, fastener fit (hole clearance), hole surface quality, type of fastener (countersunk, rivets, bolts), surface quality including coatings

or sealants and more. Two common configurations occur when referring to joints and fastener exibility, namely single shear and double shear loaded fasteners, illustrated in Figure 2.5

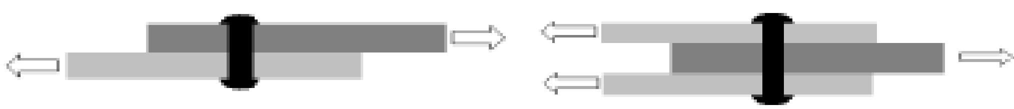

Fig 2.5 Type of shear

The fastener flexibility is a measure of the influence of fasteners (rivets, bolts, etc.) on the flexibility of the whole joints. It plays an important role when considering the factors influencing the strength level and fatigue life of an aircraft joint.

In terms of load transfer and deformation, the fasteners stiffness (flexibility) determines the way load is transferred from one component to another, and choosing the right value of stiffness is an important factor in the results of a joint analysis.

2.1 Tate

Determination of the bolt load distribution in a joint is highly dependent on fastener flexibility, i.e., the behavior of the fasteners as elastic beams. Tate and Rosenfeld derived a linear elastic theory for the loads carried by individual bolts in a joint, and in doing so created a “bolt constant”, or “correlation coefficient” C that relates the various contributions from beam mechanisms to joint flexibility. [16]

$$C_f = C_{bs} + C_{bb} + C_{bbr} + C_{pbr} \tag{2.1.1}$$

where Cbs is the shear effect; Cbb is the bending effect; Cbbr is the bearing effect; and Cpbr is the plate bearing effect, given by the following equations:

$$C_{bs} = \frac{2t_s + t_p}{3G_b A_b} \tag{2.1.2}$$

$$C_{bb} = \frac{8t_s^3 + 16t_s^2 t_p + 8t_s t_p^2 + t_p^3}{192 E_{bb} I_b} \tag{2.1.3}$$

$$C_{bbr} = \frac{2t_s + t_p}{t_s t_p E_{bbr}} \tag{2.1.4}$$

$$C_{pbr} = \frac{1}{t_s E_{sbr}} + \frac{2}{t_p E_{pbr}} \tag{2.1.5}$$

Here t_p and t_s are the thicknesses of the plate and strap, respectively, A_b is the area of the bolt$\left(\frac{\pi d^2}{4}\right)$, and Ib is the bolt moment of inertia $\left(\frac{\pi d^4}{64}\right)$. These equations are used for the single-shear joints in the wing design (rib-to-spar, rib-to-skin, and spar-to-skin). In these single-shear cases the plates and straps are composite laminates.

It was found that the linear portions of these load deflection curves could be represented accurately by minor modifications of an old NACA formula.

This is shown in Figure 2.6 for double shear, giving excellent correlation with the mean values, despite the large experimental scatter, the reason for which is not known. The stiffness formula is given as the sum of four components. Thus,

$$\frac{1}{K} = \frac{2\delta}{P} = C_{bs} + C_{bb} + C_{bbr} + C_{pbr} \tag{2.1.6}$$

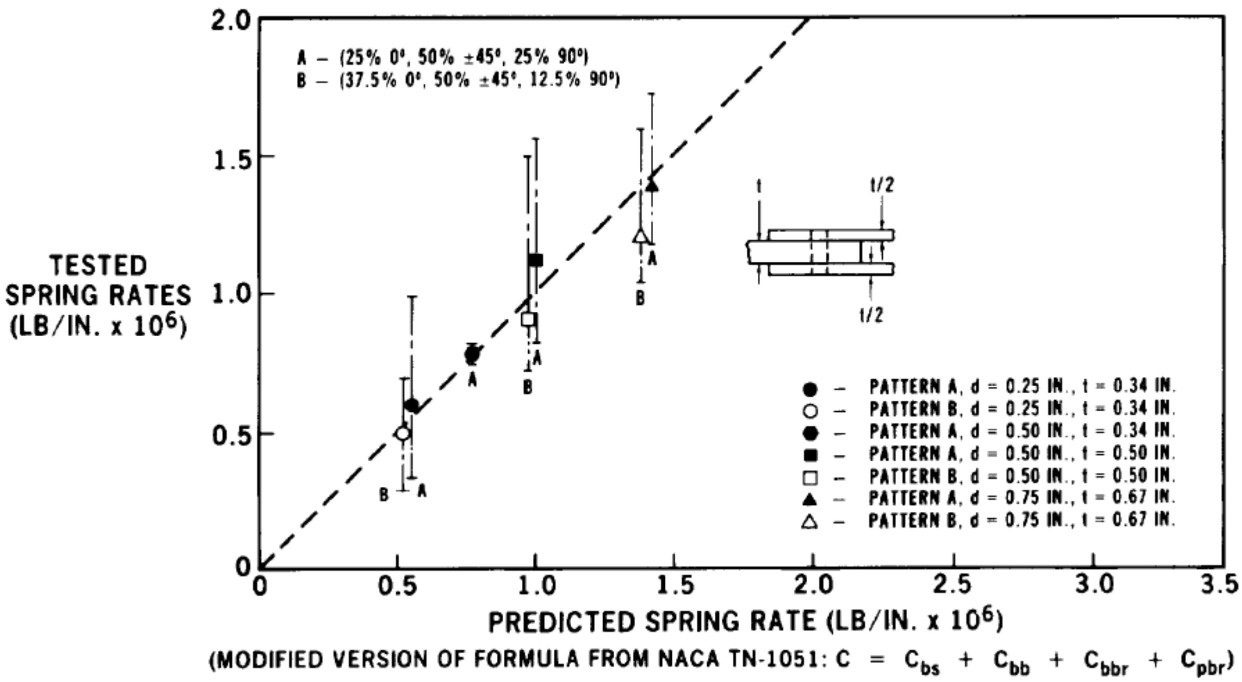

Fig 2.6 Bolted joint elastic spring rates – test versus prediction

The empirical expressions deduced by Tate and Rosenfeld for this expression give, for bolts loaded symmetrically in double shear,

$$\frac{1}{K} = \frac{2t_s+t_p}{3G_bA_b} + \frac{8t_s^3+16t_s^2t_p+8t_st_p^2+t_p^3}{192E_{bb}I_b} + \frac{2t_s+t_p}{t_st_pE_{bbr}} + \frac{1}{t_s(\sqrt{E_L*E_T})_s} + \frac{2}{t_p(\sqrt{E_L*E_T})_p} \tag{2.1.7}$$

refers to each of the splice straps (which are assumed to be identical), and p to the basic plate (or skin). The various thicknesses are given by t, as shown in Figure 2.7, and the various elastic moduli are signified by E for a Young's modulus and G for the shear modulus of the bolt,

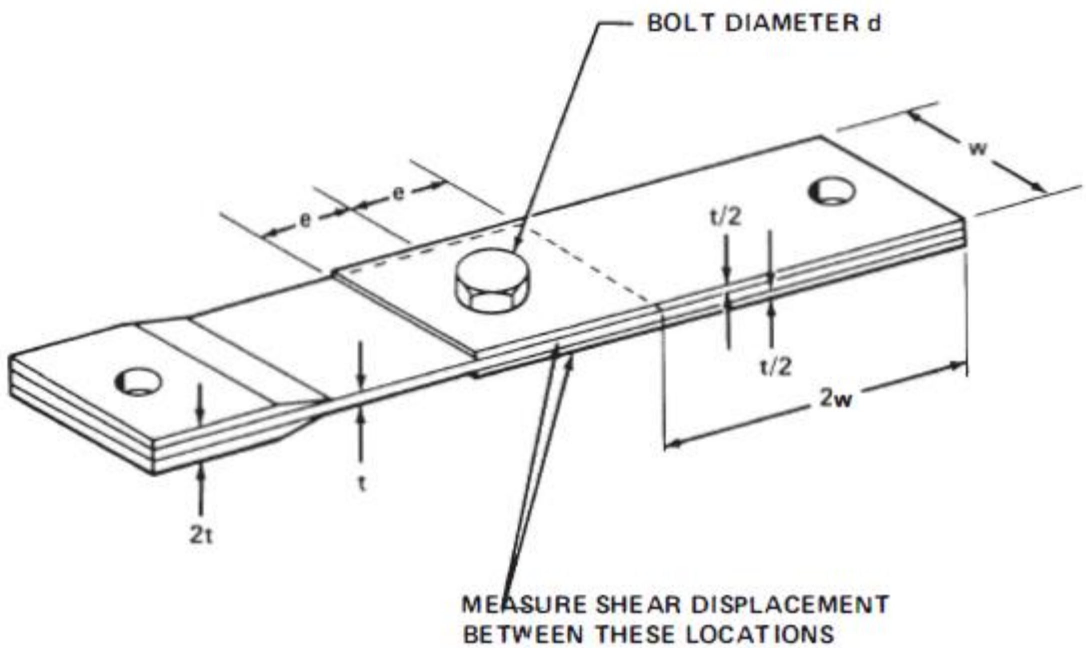

Fig 2.7 Ancillary test specimen – double shear tension

2.2 Lee

Before as Tate and Rosenfeld finalized their formal for double-shear joint, Lee started improve this equation for composite metal double shear joining. A double-shear joint with two fastener rows is shown in Figure 2.8 with relevant geometry labels.Tate and Rosenfeld equations are used for the single-shear joints in the wing design (rib-to-spar, rib-to-skin, and spar-to-skin). In these single-shear cases the plates and straps are composite laminates. In the case of the double-shear joint it was found that the NACA 1051 equations for the correlation coefficient did not represent experimental test results accurately [16]. The bolt shear, bending, and bearing deformation terms were reduced as the deformations were too large compared to the strap bearing deformation. Lee [17] modified the equations appropriately to match test observations, resulting in

$$C_{bs} = \frac{t_s + t_p}{5G_b A_b} \tag{2.2.1}$$

$$C_{bb} = \frac{L_{eff}^3}{192E_{bb}I_b} \tag{2.2.2}$$

$$C_{bbr} = \frac{3t_s + t_p}{3t_s t_p E_{bbr}} \tag{2.2.3}$$

$$C_{pbr} = \frac{1.1}{t_s\sqrt{E_{s1}E_{s2}}} + \frac{1.1}{t_p\sqrt{E_{p1}E_{p2}}} \tag{2.2.4}$$

where E_{s1} and E_{s2} are the axial and transverse Young's moduli of the strap, E_{p1} and E_{p2} are the axial and transverse Young's moduli of the plate, and L_{eff} is given as

$$L_{eff} = \frac{t_s}{3} + \frac{t_p}{5} \tag{2.2.5}$$

These equations are used in this study for the double-shear joints in the wing design (side-ofbody (SOB) skin/stringer, SOB skin/spar, and SOB rib). These joints vary in strap and plate definitions; in some cases, an average of laminate stiffnesses was taken to account for their unique design.

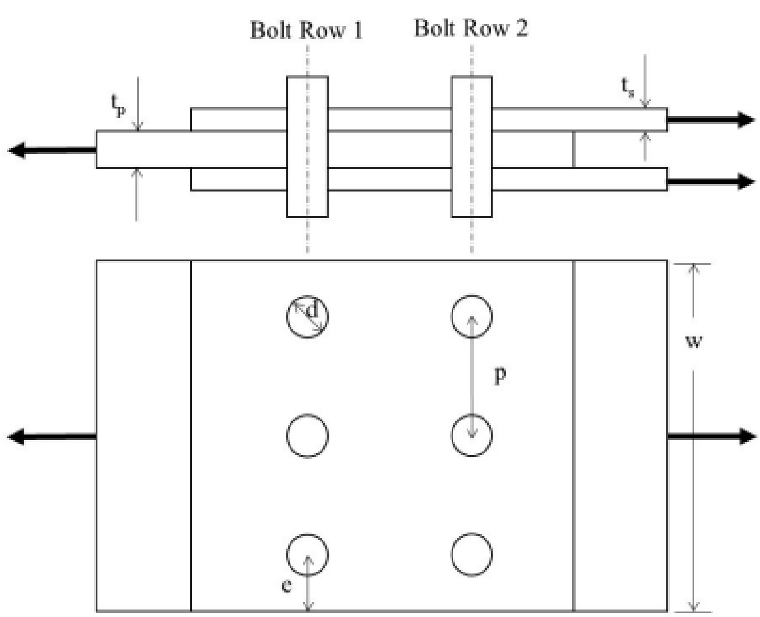

Fig 2.8 Double shear joint

For joint design automation within the optimization program there are design considerations and checks based on composite bolted joint experience and research. The first check in the design is the hole diameter to laminate thickness ratio [22]:

$$\frac{d}{tn} \geq \frac{1}{3} \tag{2.2.6}$$

2.3 Huth

Based on extensive testing on different types of joints and materials, a formula for fastener flexibility was fitted to load-displacement curves as

$$C_f = (\frac{t_p+t_s}{2d})^a * \frac{b}{n} * (\frac{1}{t_pE_p} + \frac{1}{nt_sE_s} + \frac{1}{2t_pE_f} + \frac{1}{2nt_sE_f}) \tag{2.3.1}$$

where a, b and n are parameters defining the joint type as seen in Fig 2.9.

Single shear	$n = 1$
Double shear	$n = 2$
Bolted metallic joints	$a = 2/3,\ b = 3.0$
Riveted metallic joints	$a = 2/5,\ b = 2.2$
Bolted graphite/epoxy joints	$a = 2/3,\ b = 4.2$

Fig 2.9: Huth parameters

The Huth formula is derived with a single-spring assumption, for single and double shear alike

2.4 Grumman

The equation is an empirically derived formula that was presented by the Grumman Aerospace Corporation and was used during the development of the Saab 37 Viggen aircraft, and the fastener flexibility is given by

$$C_f = \frac{(t_p+t_s)^2}{E_f d^3} + 3.7 * (\frac{1}{t_p E_p} + \frac{1}{t_s E_s}) \quad (2.4.1)$$

The conditions under which the testing was performed, that eventually lead up to the Grumman formula, is unclear. Nordin [18] claims it was derived for metallic materials, for which both bolts and rivets can be used in joining plates. It was however used during the development of a composite component for the Viggen aircraft [19], which are usually not joined by rivets. The formula does however not account for fastener tightening, hole clearance, and whether the fastener is countersunk or not [18].

2.5 Barrois

The method by Barrois was developed using an analytical approach by modeling the fastener as a beam on an elastic foundation, taking into account bending and shearing deflections of the fastener. The assumption is made that there is a linear relation between the deflection of the fastener and the applied load. Also, it is assumed there is no clearance between fastener and foundation. Both single shear and double shear loaded fastener installations are handled.

In the derivation it is assumed that the joined plates are of the same material. Finally, two different boundary conditions are applied at the fastener ends, yielding several ways of using Barrois' method (`variants'). These boundary conditions are clamped fastener heads (bolts) and free fastener heads (pins). Barrois uses a single-spring assumption, similar to Huth. In addition, in calculating load distribution, Barrois attempts to take into account holes in plates.

The Barrois derivation of the fastener flexibility is quite extensive and not reproduced in detail in this report. The interested reader may find a detailed description of the method by Barrois in Reference [20].

2.6 Basic Compatibility-Equilibrium Method

[27] In the discussion that follows, one plate is designated with subscript “s” (indicating “strap”) and the other plate with subscript “p”. In the compatibility/equilibrium method there is a strict definition of plate and strap, illustrated in **Ошибка! Источник ссылки не найден.**. The strap represents the outer members in a double-shear joint. In a single- or double-shear hardpoint, the strap is the discontinuous hardpoint member, while the plate is the member through which the remote load enters the joint.

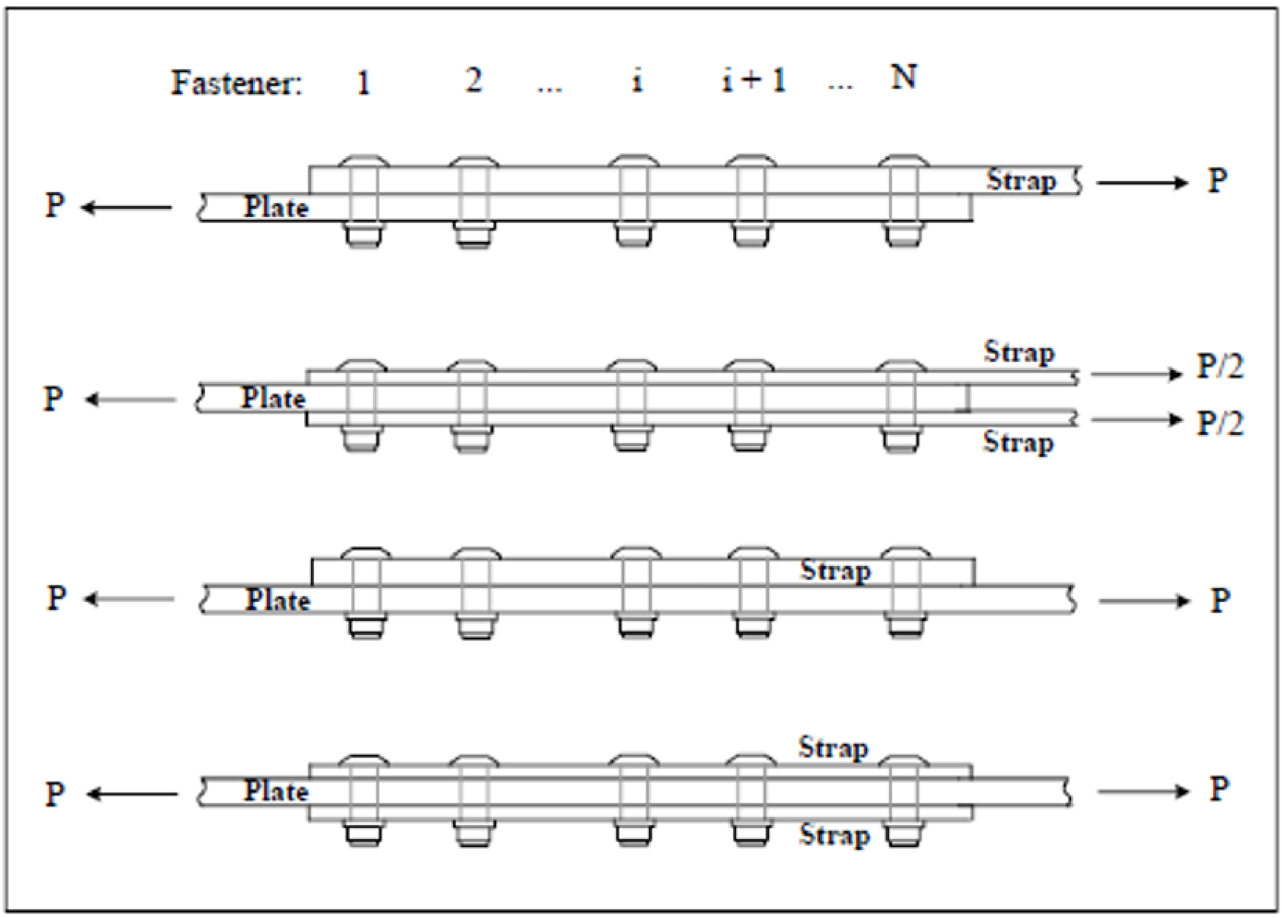

Fig 2.10 Terminology of Plate and Strap in the Compatibility/Equilibrium Method

The joint has *N* rows. Fasteners are numbered sequentially 1 through *N*. The plate load enters the joint at fastener #1, and the strap begins (has a free edge) at fastener #1.

A section of the joint, including two adjacent fasteners and the connecting plates, is isolated from the spring model, as shown in **Ошибка! Источник ссылки не найден.**. Deformation compatibility between points A and B states that the sum of the fastener I deformation ($\delta_{f,i}$) and strap deformation ($\delta_{s,i}$) equals the sum of the plate deformation ($\delta_{p,i}$) and the fastener i+1 deformation ($\delta_{f,(i+1)}$):

$$\delta_{f,i} + \delta_{s,i} = \delta_{p,i} + \delta_{f,(i+1)} \qquad (2.6.1)$$

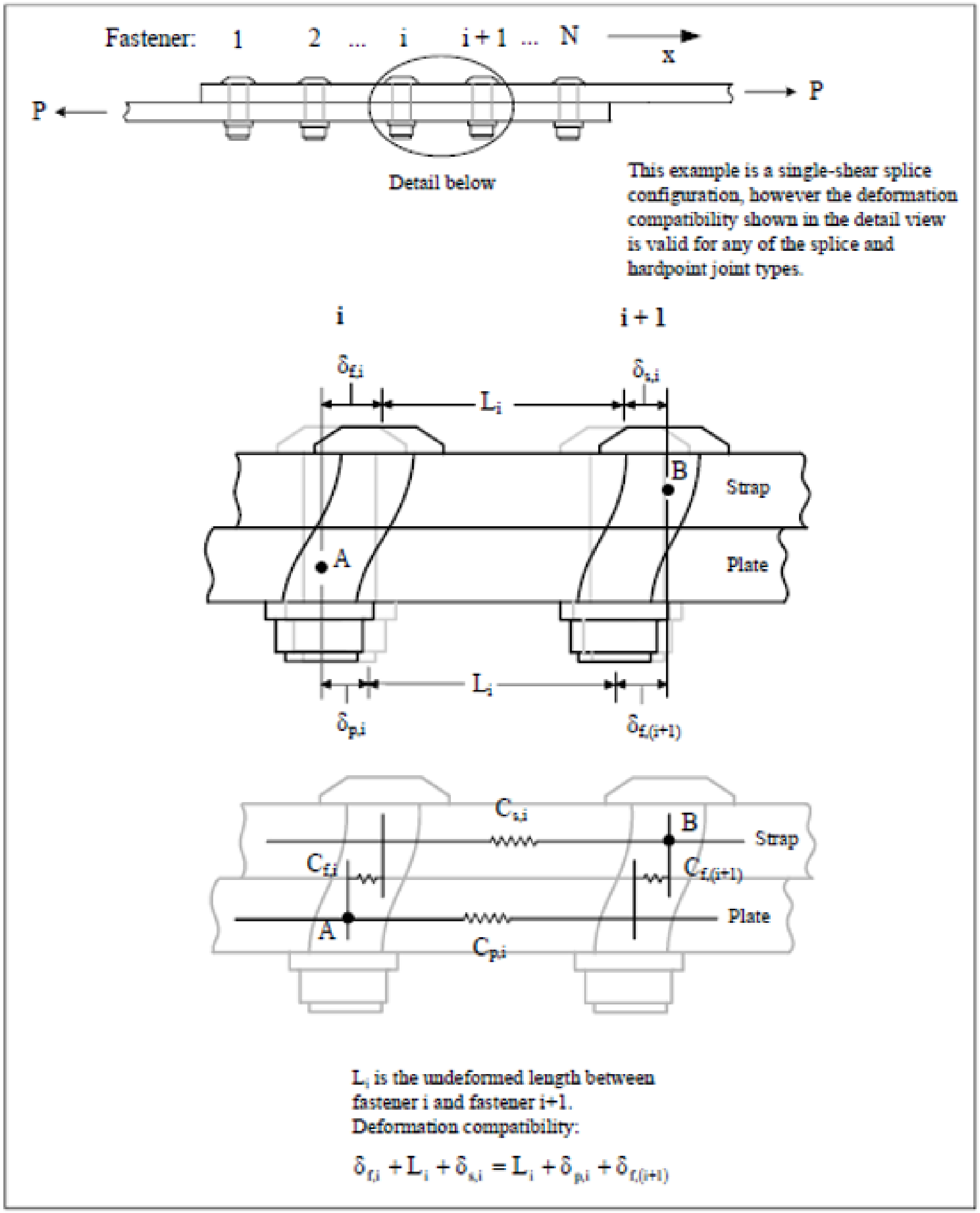

Fig 2.11 Deformation Compatibility between Two Adjacent Fasteners

The definition of fastener flexibility C_f is the deformation of the fastener divided by the load transferred across the fastener shear plane. Solving for deformation, for i^{th} fastener,

$$\delta_{f,i} = \left(\frac{R_i}{k}\right) C_{f,i} \tag{2.6.2}$$

Where

k=1 – for single shear

k=2 – for double symmetrical shear

Where R is the load transferred across the fastener shear plane and $C_{f,I}$ is the flexibility of the i^{th} fastener element. Note that in double-shear configurations R_i is the total load transferred through both shear planes. The definition of k (1 for single-shear, 2 for symmetric double shear) holds throughout this derivation.

For the i^{th} plate element, flexibility $C_{p,I}$ is the deformation of the plate element divided by the load in the load in the plate element, therefore:

$$\delta_{p,i} = P_{p,i} C_{p,i} \ , \quad \text{and similarly} \quad \delta_{s,i} = P_{s,i} C_{s,i} \tag{2.6.3}$$

The load in the i^{th} plate element in the plate ($P_{p,i}$) and strap ($P_{s,i}$) can be determined by taking a free body of the plate and strap, cut between the i^{th} and $(i+1)^{th}$ fasteners. These free bodies are shown in **Ошибка! Источник ссылки не найден.**. In the strap,

$$P_{s,i} = \sum_{j=1}^{i} \left(\frac{R_j}{k}\right) \tag{2.6.4}$$

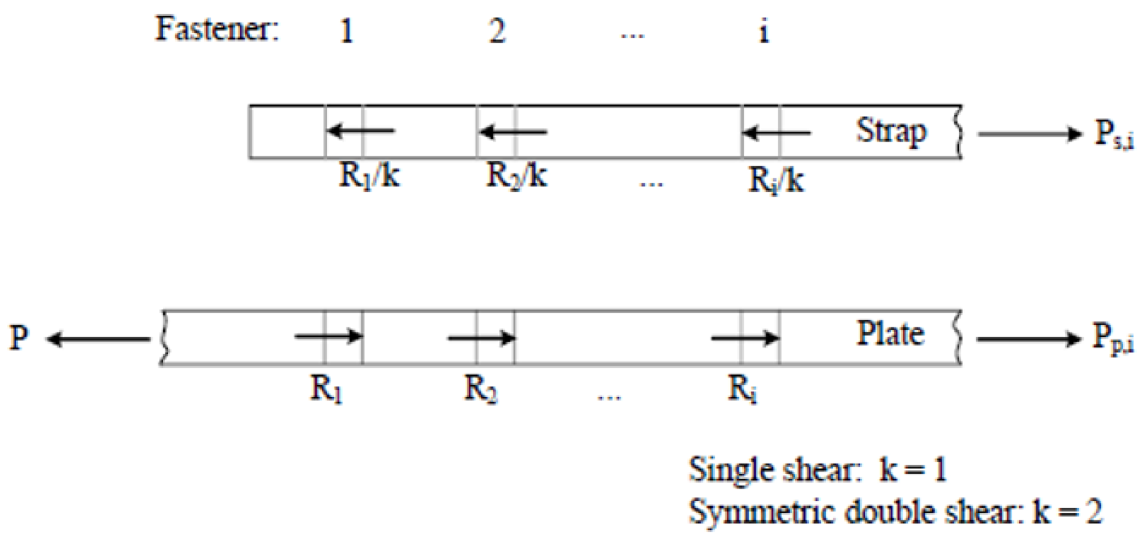

Fig 2.12 A free body of the plates cut past the i[th] fastener

In a hardpoint, under a positive tensile load P, load transferred from the plate to strap is assigned a positive value, and load transferred from the strap to plate is assigned a negative value. A negative compressive load P reverses the sign of the R_i fastener loads. (**Ошибка! Источник ссылки не найден.**2.12 shows the positive sign convention). The following equation shows the function of the unknown fastener loads (R_1 through R_i), the plate and fastener flexibility, and the applied load P:

$$\left(\frac{R_i}{k}\right) C_{f,i} + \left[\sum_{j=1}^{i} \left(\frac{R_j}{k}\right)\right] C_{s,i} = \left(P - \sum_{j=1}^{i} R_j\right) C_{p,i} + \left(\frac{R_{(i+1)}}{k}\right) C_{f,(i+1)} \qquad (2.6.5)$$

Collecting the fastener load terms and dividing by the plate i flexibility,

$$\left(\frac{C_{f,i}+C_{s,i}}{kC_{p,i}} + 1\right) R_i + \left(\frac{C_{s,i}}{kC_{p,i}} + 1\right) \sum_{j=1}^{(i-1)} R_j - \left(\frac{C_{f,(i+1)}}{kC_{p,i}}\right) R_{(i+1)} = P \qquad (2.6.6)$$

This equation may be written for each pair of adjacent fasteners, for a total of (N-1) equations, where N is the number of fastener rows in the single-column joint.

One additional equation can be written according to equilibrium of load in the joint, using a free body similar to **Ошибка! Источник ссылки не найден.**2.12. In a lap joint, the sum of the loads across the fastener shear planes must balance the incoming load P. In a hardpoint, the incoming and outgoing loads in the strap must sum to zero. The equations above can be assembles into a matrix that can be solved for the fastener loads R_i:

$$\begin{bmatrix} D_1 & B_1 & 0 & 0 & \cdots & 0 & 0 \\ A_2 & D_2 & B_2 & 0 & \cdots & 0 & 0 \\ A_3 & A_3 & D_3 & B_3 & \cdots & 0 & 0 \\ \vdots & \vdots & \vdots & \vdots & \cdots & \vdots & \vdots \\ A_{(N-1)} & A_{(N-1)} & A_{(N-1)} & A_{(N-1)} & \cdots & D_{(N-1)} & B_{(N-1)} \\ 1 & 1 & 1 & 1 & \cdots & 1 & 1 \end{bmatrix} \begin{bmatrix} R_1 \\ R_2 \\ R_3 \\ R_4 \\ \vdots \\ R_{(N-1)} \\ R_N \end{bmatrix} = \begin{bmatrix} P \\ P \\ P \\ \vdots \\ P \\ \langle 0 \text{ or } P \rangle \end{bmatrix}$$

(The last row of the right-hand side is 0 for a hardpoint, and P for a lap joint).

Term is the matrix are:

$$A_i = \frac{C_{s,i}}{kC_{p,i}} \tag{2.6.7}$$

$$B_i = \frac{-C_{f,(i+1)}}{kC_{p,i}} \tag{2.6.8}$$

$$D_i = \frac{C_{f,i}+C_{s,i}}{kC_{p,i}} + 1 \tag{2.6.9}$$

Where k = 1 for single-shear joints, and k = 2 for symmetric double-shear joints.[27]

3. DETERMINATION OF THE STIFFNESS MATRIX OF A PACKAGE OF MONOLAYERS

Composite material, also called composite, a solid material that results when two or more different substances, each with its own characteristics, are combined to create a new substance whose properties are superior to those of the original components in a specific application. The term composite more specifically refers to a structural material (such as plastic) within which a fibrous material (such as silicon carbide) is embedded.

Composites, also known as Fiber-Reinforced Polymer (FRP) composites, are made from a polymer matrix that is reinforced with an engineered, man-made or natural fiber (like glass, carbon or aramid) or other reinforcing material. The matrix protects the fibers from environmental and external damage and transfers the load between the fibers. The fibers, in turn, provide strength and stiffness to reinforce the matrix—and help it resist cracks and fractures [21].

To identify any monolayer in the monolayer package, a layer orientation code is used that defines:

- the angle of inclination of the monolayer to the base axis of the package of monolayers X;
- the number of monolayers having a given angle of inclination;
- exact arrangement of monolayers.

The number showing the orientation of monolayer in degrees between the direction of its fibers and the axis X. indicated each monolayer The standard orientation of monolayers is 0°, +45°, -45° и 90°. Fig 3.1

An oblique line separates adjacent monolayers, if their angles of inclination are different. Adjacent monolayers having the same angle are denoted by a digital subscript.

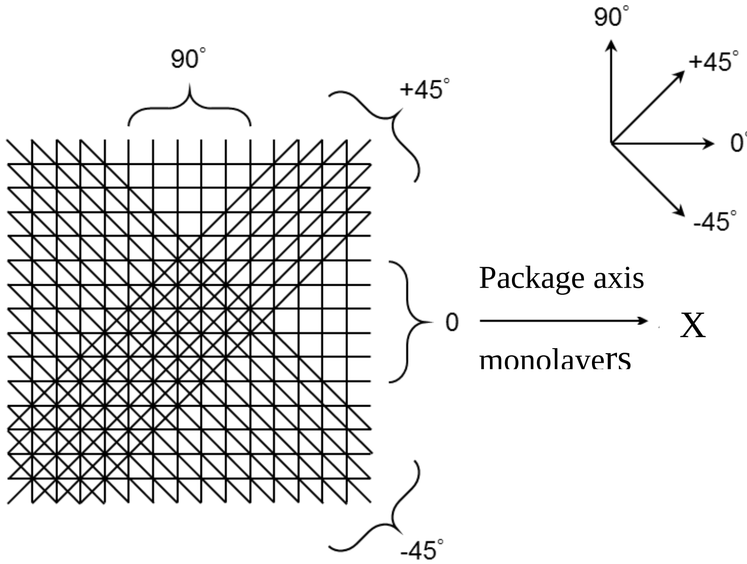

Fig 3.1 standard orientation of monolayers

The subscript “T” at the bracket indicates that the complete package of monolayers is given.

Sometimes instead of the negative angles of the first quadrant, the positive angles found in the second quadrant are used. For example, instead of designating an angle of -45°, the designation 135 ° is used.

Elastic properties of carbon monolayer Table 3.1

Table 3.1 – Elastic property

Monolayer	Modules of elasticity and shear, ksi			Poisson's ratios	
	E_1	E_2	G_{12}	μ_{12}	μ_{21}
Tape	20740	1218	812	0.36	0.02
Fabric	9427	9137	943	0.070	0.068

Stiffness Matrix Coefficients

$$C_{11}^{0} = \frac{E_1}{1-\mu_{12}\cdot\mu_{21}} \tag{3.1}$$

$$C_{12}^{0} = \frac{E_1\cdot\mu_{21}}{1-\mu_{12}\cdot\mu_{21}} = \frac{E_2\cdot\mu_{12}}{1-\mu_{12}\cdot\mu_{21}} \tag{3.2}$$

$$C_{22}^{0} = \frac{E_2}{1-\mu_{12}\cdot\mu_{21}} \tag{3.3}$$

$$C_{66}^{0} = G_{12} \tag{3.4}$$

Where

E_1, E_2 – longitudinal and transverse elastic modules of a monolayer.

G_{12} – Shear modules of a monolayer.

μ_{12} – Principal Poisson’s ratio.

μ_{21} – Secondary Poisson's ratio, determined from the Maxwell relation:

$$\mu_{12}\cdot E_2 = \mu_{21}\cdot E_1 \tag{3.5}$$

Independent coefficients

$$V_1 = \left(3\cdot C_{11}^{0} + 2\cdot C_{12}^{0} + 3\cdot C_{22}^{0} + 4\cdot C_{66}^{0}\right)/8 \tag{3.6}$$

$$V_2 = \left(C_{11}^{0} - C_{22}^{0}\right)/2 \tag{3.7}$$

$$V_3 = \left(C_{11}^{0} - 2\cdot C_{12}^{0} + C_{22}^{0} - 4\cdot C_{66}^{0}\right)/8 \tag{3.8}$$

$$V_4 = \left(C_{11}^{0} - 2\cdot C_{12}^{0} + C_{22}^{0} + 4\cdot C_{66}^{0}\right)/8 \tag{3.9}$$

Coefficients of the stiffness matrix of a monolayer rotated by an angle ϕ

$$C_{11}^{\varphi} = V_1 + V_2 \cdot \cos 2\varphi + V_3 \cdot \cos 4\varphi \tag{3.10}$$

$$C_{12}^{\varphi} = V_1 - 2 \cdot V_4 - V_3 \cdot \cos 4\varphi \tag{3.11}$$

$$C_{16}^{\varphi} = 0.5 \cdot V_2 \cdot \sin 2\varphi + V_3 \cdot \sin 4\varphi \tag{3.12}$$

$$C_{22}^{\varphi} = V_1 - V_2 \cdot \cos 2\varphi + V_3 \cdot \cos 4\varphi \tag{3.13}$$

$$C_{26}^{\varphi} = 0.5 \cdot V_2 \cdot \sin 2\varphi - V_3 \cdot \sin 4\varphi \tag{3.14}$$

$$C_{66}^{\varphi} = V_4 - V_3 \cdot \cos 4\varphi \tag{3.15}$$

Elastic characteristics for angels ϕ

$$E_x = C_{11} - \frac{C_{12}^2}{C_{22}} \qquad \text{(XX)}$$

$$E_y = C_{22} - \frac{C_{12}^2}{C_{11}} \qquad \text{(XX)}$$

$$G_{xy} = C_{66} \qquad \text{(XX)}$$

$$G_{xy} = C_{66} \qquad \text{(XX)}$$

Table 3.2 Fabric coefficient of the stiffness

φ,°	C_{11}	C_{12}	C_{16}	C_{22}	C_{26}	C_{66}
0	9472	642.67	0	9181	0	942.75
±5	9368	745.17	593.96	9080.7	-568.7	1045.2
±10	9066	1040.3	1117.4	8792.1	-1068	1340.4
±15	8603	1492.5	1508.4	8350.7	-1435	1792.6
±20	8034	2047.2	1720.7	7810.6	-1627	2347.2
±25	7426	2637.4	1729.6	7238.3	-1618	2937.5
±30	6850	3192.1	1535	6704.4	-1409	3492.2
±35	6375	3644.3	1161	6275.2	-1024	3944.4
±40	6055	3939.4	653.07	6004.6	-509.6	4239.5
±45	5927	4041.9	72.865	5927.4	72.865	4342
±50	6005	3939.4	-509.6	6055.2	653.07	4239.5
±55	6275	3644.3	-1024	6374.9	1161	3944.4
±60	6704	3192.1	-1409	6850.1	1535	3492.2
±65	7238	2637.4	-1618	7425.6	1729.6	2937.5
±70	7811	2047.2	-1627	8033.8	1720.7	2347.2
±75	8351	1492.5	-1435	8603.1	1508.4	1792.6
±80	8792	1040.3	-1068	9066	1117.4	1340.4
±85	9081	745.17	-568.7	9367.7	593.96	1045.2
±90	9181	642.67	-4E-13	9472.4	4E-13	942.75

Table 3.3 Tape coefficient of the stiffness

φ,°	C_{11}	C_{12}	C_{16}	C_{22}	C_{26}	C_{66}
0	20900	441.96	0	1227.7	0	812.21
±5	20614	577.61	1623.3	1241.4	84.689	947.86
±10	19780	968.19	3127.9	1294.6	236.22	1338.4
±15	18457	1566.6	4406.9	1420.8	511.03	1936.9
±20	16740	2300.7	5376.3	1670.1	946.08	2670.9
±25	14746	3081.8	5982.5	2101.3	1552.2	3452.1
±30	12608	3815.9	6207	2771.7	2311.1	4186.2
±35	10455	4414.3	6067.2	3727.1	3175.5	4784.6
±40	8409	4804.9	5612.6	4992.6	4073.9	5175.2
±45	6565	4940.6	4918	6565	4918	5310.8
±50	4993	4804.9	4073.9	8408.6	5612.6	5175.2
±55	3727	4414.3	3175.5	10455	6067.2	4784.6
±60	2772	3815.9	2311.1	12608	6207	4186.2
±65	2101	3081.8	1552.2	14746	5982.5	3452.1
±70	1670	2300.7	946.08	16740	5376.3	2670.9
±75	1421	1566.6	511.03	18457	4406.9	1936.9
±80	1295	968.19	236.22	19780	3127.9	1338.4
±85	1241	577.61	84.689	20614	1623.3	947.86
±90	1228	441.96	5E-14	20900	1E-12	812.21

Table 3.4 Change in the elastic characteristics depending on the angle φ° of a fabric monolayer in the coordinate system

φ,°	$E_{x,}$ ksi	$E_{y,}$ ksi	$G_{xy,ksi}$	μ_{xy}
±0	9427	9137	943	0.07
±5	9307	9021	1045	0.08
±10	8943	8673	1340	0.12
±15	8336	8092	1793	0.18
±20	7497	7289	2347	0.26
±25	6465	6301	2938	0.36
±30	5330	5217	3492	0.48
±35	4259	4192	3944	0.58
±40	3471	3442	4240	0.66
±45	3171	3171	4342	0.68
±50	3442	3471	4240	0.65
±55	4192	4259	3944	0.57
±60	5217	5330	3492	0.47
±65	6301	6465	2938	0.36
±70	7289	7497	2347	0.25
±75	8092	8336	1793	0.17
±80	8673	8943	1340	0.11
±85	9021	9307	1045	0.08
±90	9137	9427	943	0.07

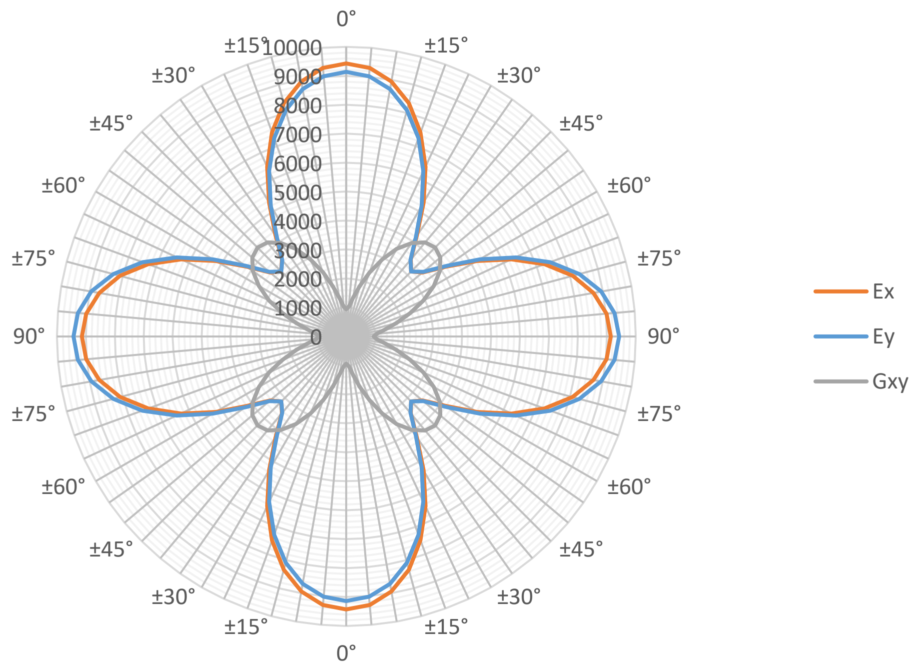

Fig 3.2 Elastic Modules and Shear module of fabric in the polar coordinate system

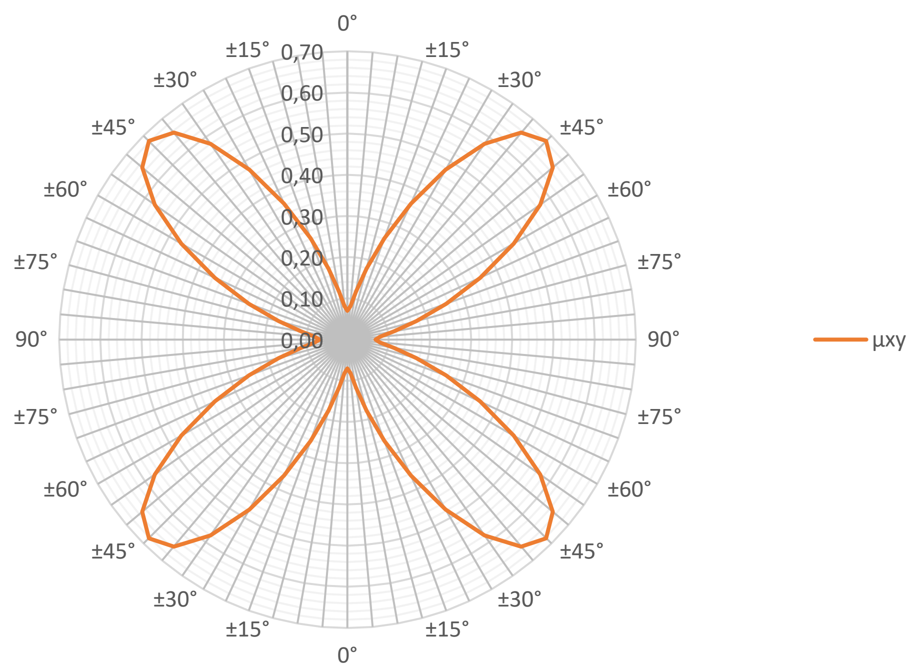

Fig 3.3 Poisson's ratio of fabric in the polar coordinate system

Table 3.5 Change in the elastic characteristics depending on the angle φ° of a tape monolayer in the coordinate system

φ,°	$E_{x,}$ ksi	$E_{y,}$ ksi	$G_{xy,ksi}$	μ_{xy}
±0	20740	1218	812	0.36
±5	20346	1225	948	0.47
±10	19056	1247	1338	0.75
±15	16730	1288	1937	1.10
±20	13570	1354	2671	1.38
±25	10226	1457	3452	1.47
±30	7354	1617	4186	1.38
±35	5227	1863	4785	1.18
±40	3784	2247	5175	0.96
±45	2847	2847	5311	0.75
±50	2247	3784	5175	0.57
±55	1863	5227	4785	0.42
±60	1617	7354	4186	0.30
±65	1457	10226	3452	0.21
±70	1354	13570	2671	0.14
±75	1288	16730	1937	0.08
±80	1247	19056	1338	0.05
±85	1225	20346	948	0.03
±90	1218	20740	812	0.02

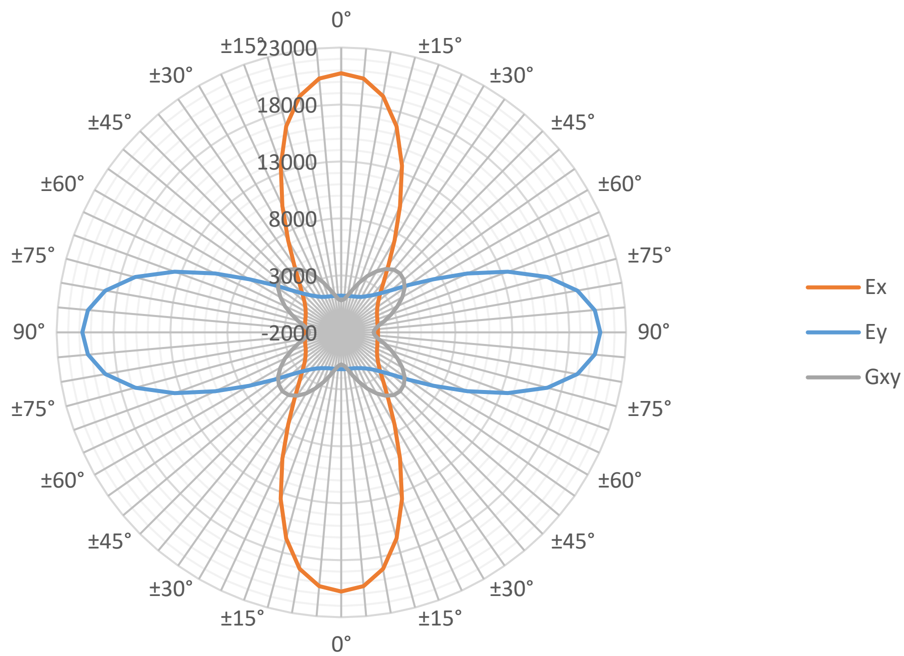

Fig 3.4 Elastic Modules and Shear module of type in the polar coordinate system

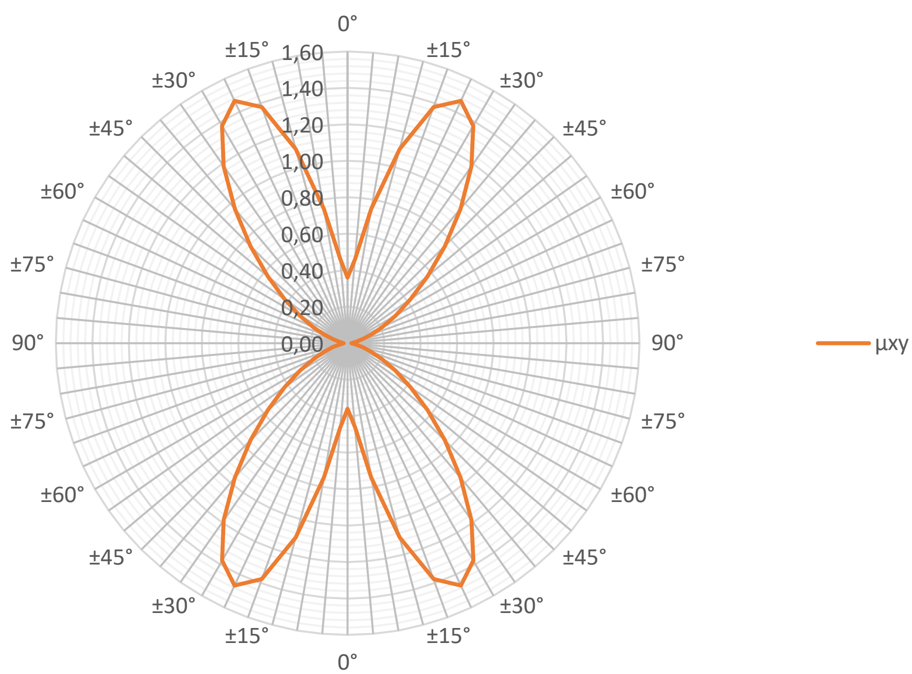

Fig 3.5 Poisson's ratio of tape in the polar coordinate system

4. STUDY OF THE INFLUENCE OF VARIOUS PARAMETERS ON THE DISTRIBUTION OF FORCES IN FASTENERS

4.1 Choosing a method of calculating flexibility

In the modern world in the production of composite structures, the more common method is laying composite layers at a certain angle, and then cutting the necessary part from this package. This method is costly because it has excess waste.

In this paper, we will consider the method of winding the composite (see fig.4.1) and its further bonding (see fig 4.2). Examples of wound carbon fiber structures are 787 fuselage, An-70 plumage, missile bodies, wind turbine blades

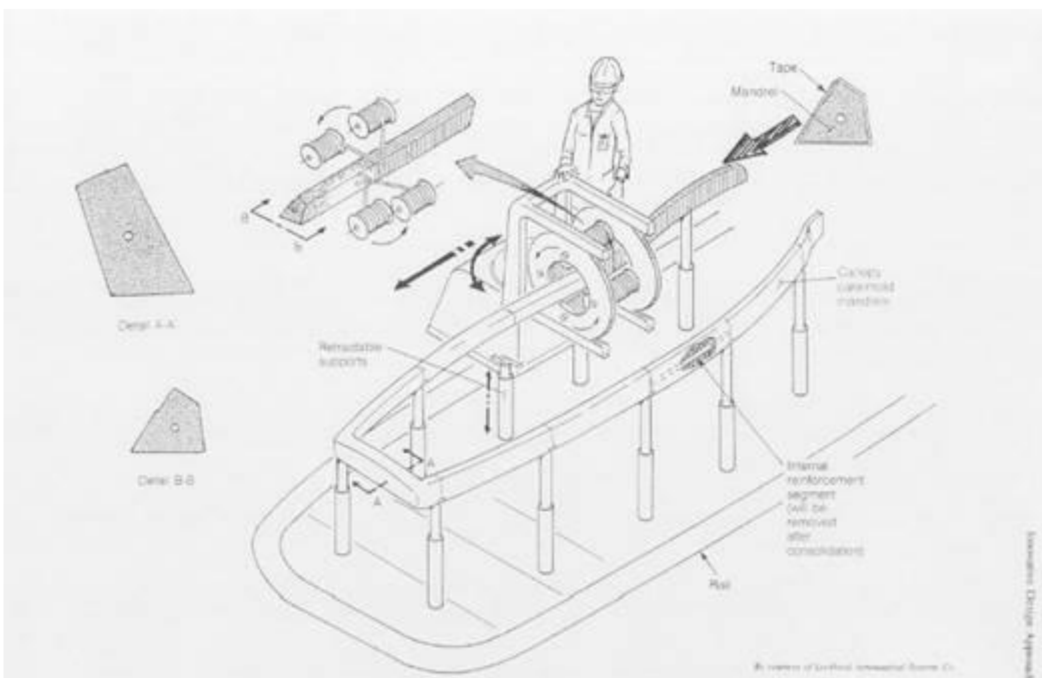

Fig 4.1 composite winding method

For further optimization, you should choose the method that gives the most accurate data. A comparison will be made for 5 cases, with different number of fasteners.
To do this, compare the data of the methods already considered and compare them with the reference data of the program.

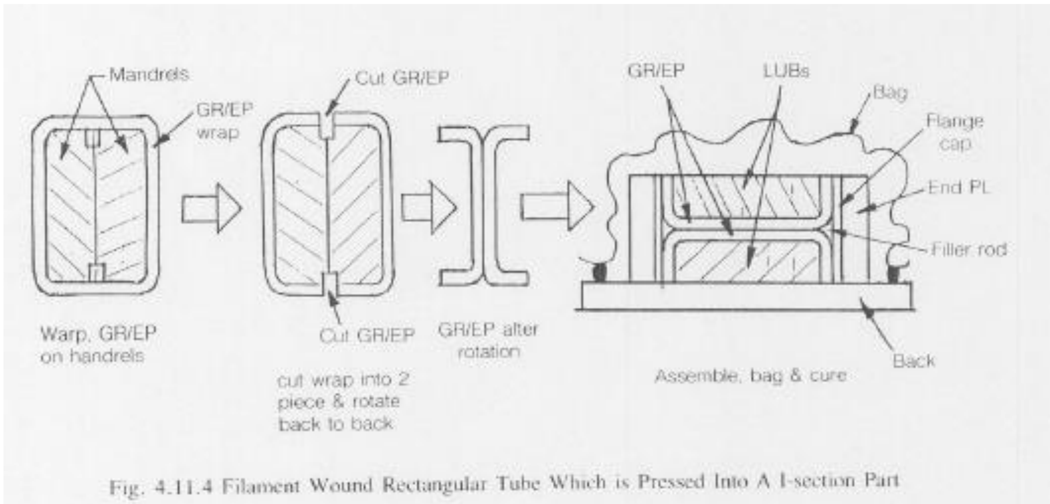

Fig 4.2 Filament wound rectangular tube which is pressed into a I-section part

To compare different methods, we use the same source data:

Fastener diameter:

D = 0.375 in

Width:

b_s, b_p = 1.875 in

Thickness:

t_s, t_p = 0.148 in

Elastic modules

E_f =1.6E7 psi; E_s=1.0E7 psi; E_p =8.6E6 psi

Pitch: 1.875 in

Flexibility: C_f, C_s, C_p – determined value

Load distribution for six fasteners

Table 4.1 Percentage distribution load for six fasteners

% \ №	1	2	3	4	5	6
Huth	36.3	18.5	10.5	8.0	9.8	16.8
Tate	37.6	18.3	9.9	7.5	9.5	17.2
Grumman	33.6	18.8	11.6	9.2	10.6	16.2
Tate&Rosenfeld	44.2	17.3	7.9	5.6	8.4	18.6
Lee	43.4	16.9	7.4	5.2	8.1	19.0
Program X	35.4	18.6	10.9	8.4	10.1	16.6

With the same thickness of the plates and straps, 1ths bolts take the greatest load, then the load goes down, on the last bolts, the load starts to increase slightly, but at the same time it does not reach such values that we can observe in loading 1ths bolts.

Different between more loaded and less loaded fasteners varies depending on the methods at 24 to 36 percent.

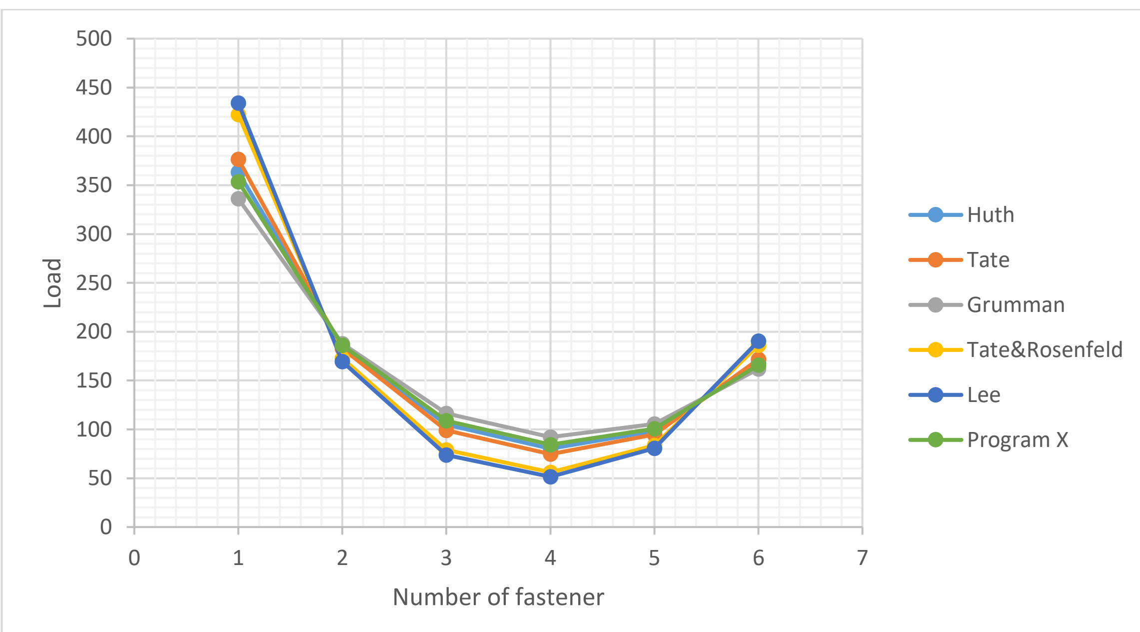

Fig 4.3 Load distribution for six bolts

Load distribution for five fasteners

Table 4.2 Percentage distribution load for five fasteners

% \ №	1	2	3	4	5
Huth	30.6	17.9	13.3	14.9	23.3
Tate	31.5	17.5	12.7	14.5	23.8
Grumman	34.6	20.1	13.9	13.3	18.1
Tate&Rosenfeld	42.6	18.1	9.7	10.1	19.5
Lee	43.8	17.6	9.1	9.7	19.8
Program X	36.2	19.8	13.1	12.6	18.3

As in the previous case, significant part of the load carried by the 1th fastener, and the general view of the graph resembles a cropped parabola.

Different between more loaded and less loaded fasteners varies depending on the methods at 17 to 34 percent.

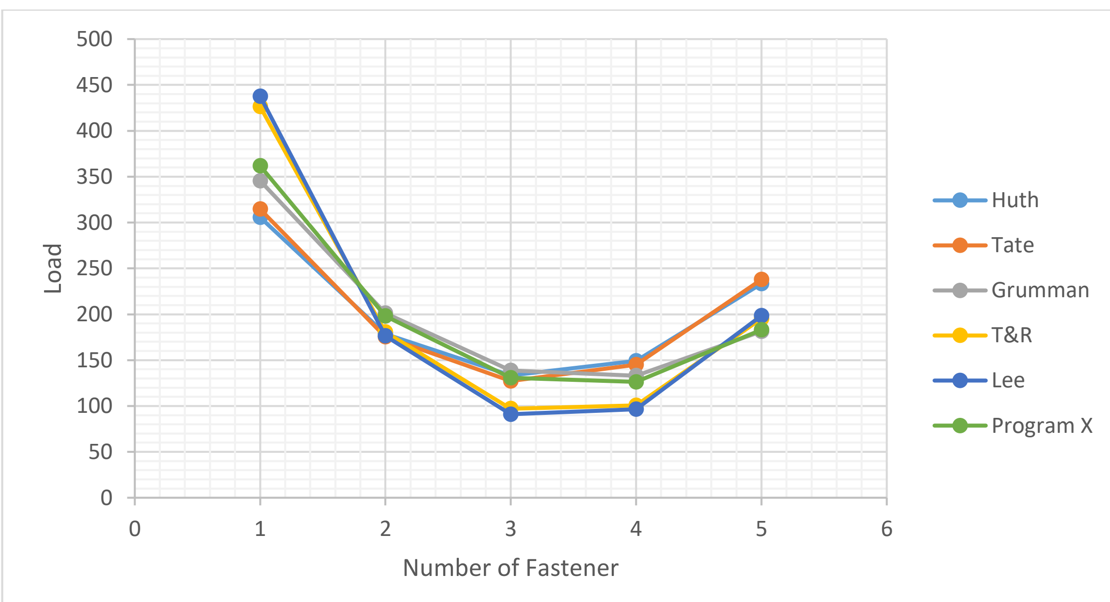

Fig 4.4 Load distribution for five bolts

Load distribution for four fasteners

Table 4.3 Percentage distribution load for four fasteners

% \ №	1	2	3	4
Huth	38.7	22.2	17.4	21.7
Tate	39.8	21.8	16.7	21.7
Grumman	36.5	22.9	18.6	21.9
Tate&Rosenfeld	43.7	20.0	14.4	21.8
Program X	37.95	22.45	17.81	21.8

As in the two previous cases, most loaded bolt is 1th. But on the last bolt it is not growing so much, does not even reach the size of the 2nd bolt.

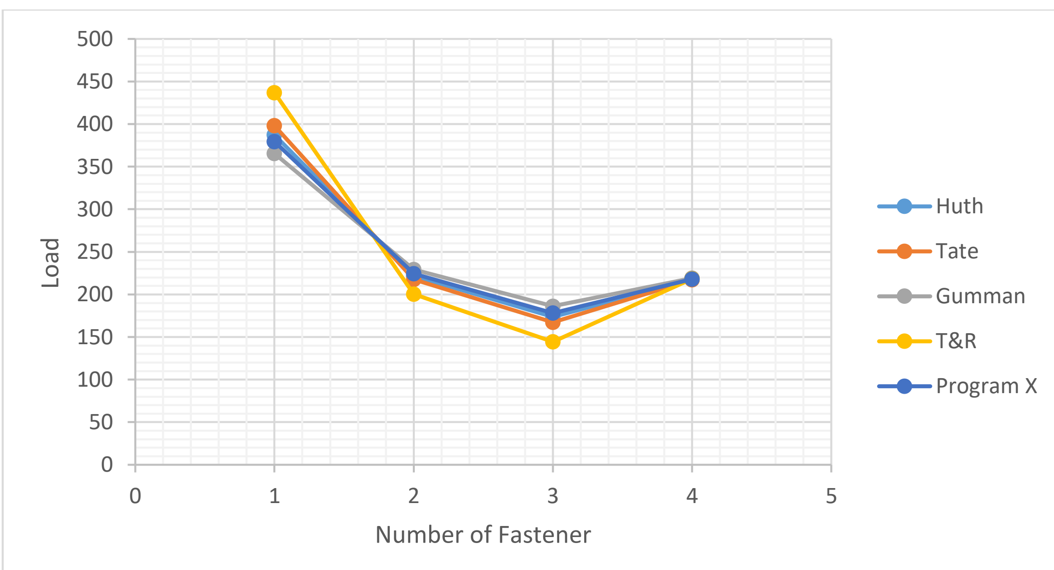

Fig 4.5 Load distribution for four bolts

Load distribution for three fasteners

Table 4.4 Percentage distribution load for three fasteners

% \ №	1	2	3
Huth	42.7	28.3	28.9
Tate	43.6	27.8	28.6
Grumman	41.1	29.3	29.5
Tate&Rosenfeld	46.6	25.6	27.7
Program X	42.2	28.7	29.1

In this case, the 1st bolt takes up almost half the entire load, the difference in the loading of the 2nd and 3rd bolt is not so significant, the curve no longer resembles a parabola.

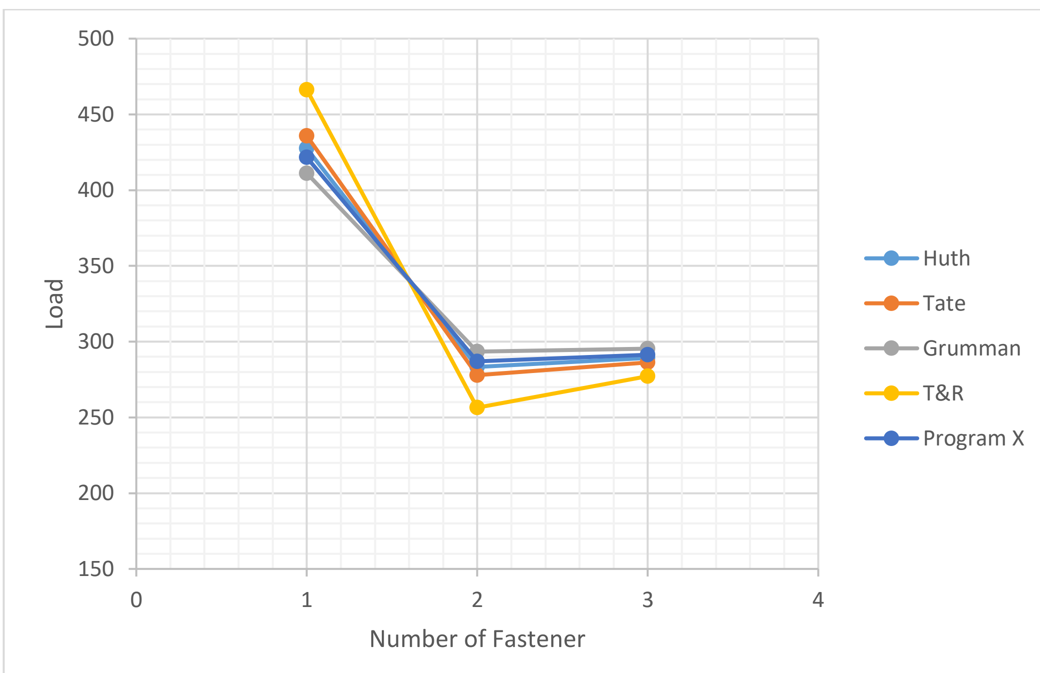

Fig 4.6 Load distribution for three bolts

Load distribution for two fasteners

Table 4.5 Percentage distribution load for three fasteners

% \ №	1	2
Huth	51.5	48.5
Tate	51.7	48.3
Grumman	53.4	46.6
Tate&Rosenfeld	56.2	43.8
Program X	53.9	46.1

When considering 2 bolts, distinction between different method extremely small.

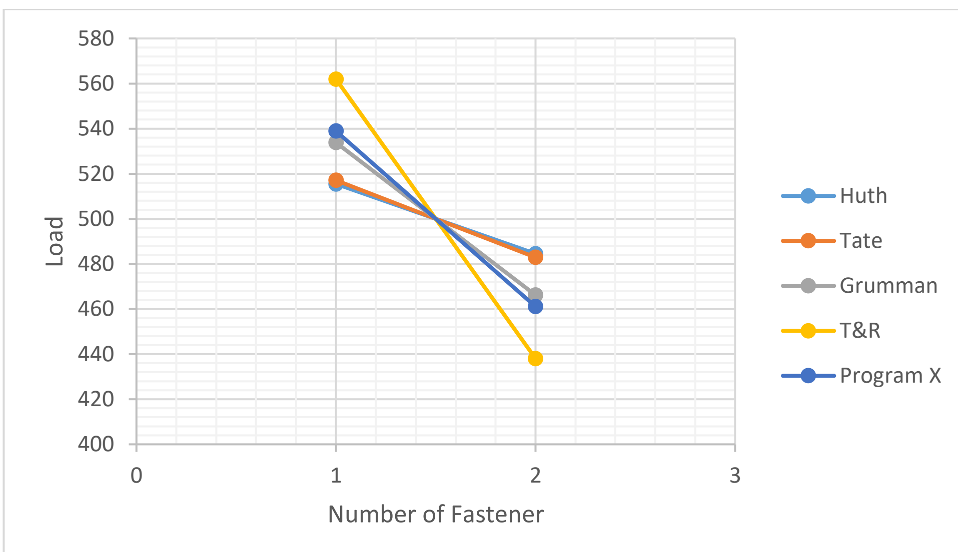

Fig 4.7 Load distribution for two bolts

For further optimization, we will use the Huth method, because it is this method that is more approximate, to the creative program for calculating metal-composite double shear joint.

4.2 Examination and selection of the modulus of elasticity

4.2.1 The dependence of the load distribution depending on the angle of inclination for fabric:

1.

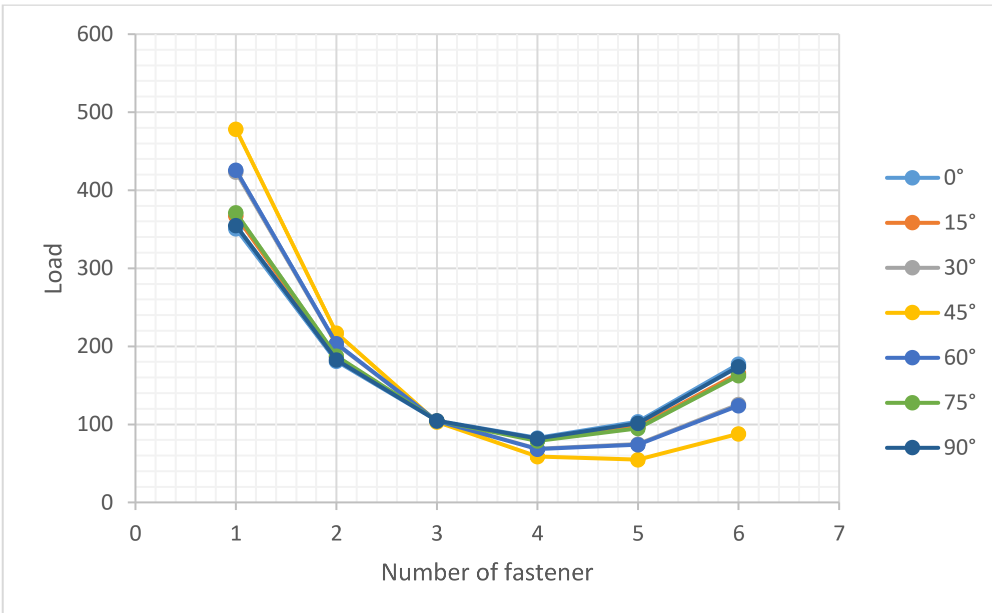

Fig 4.9 for six fasteners

2.

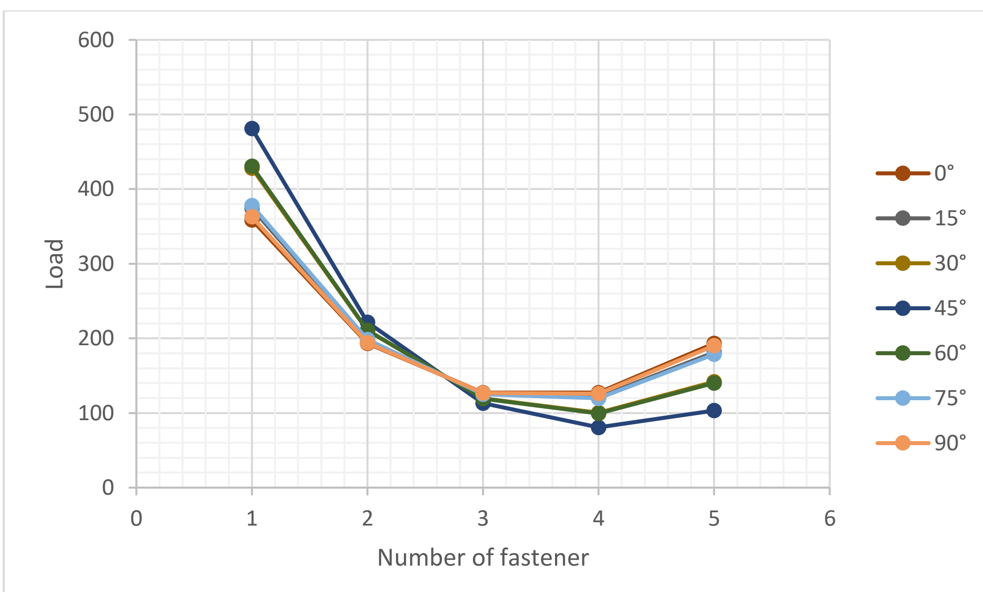

Fig 4.9 for five fasteners

3.

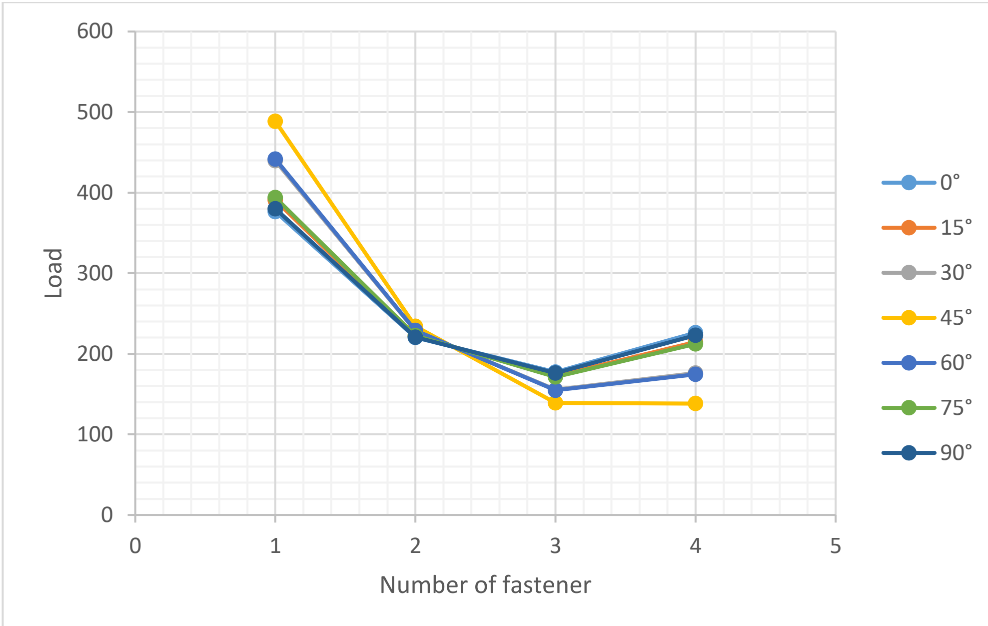

Fig 4.10 for four fasteners

4.

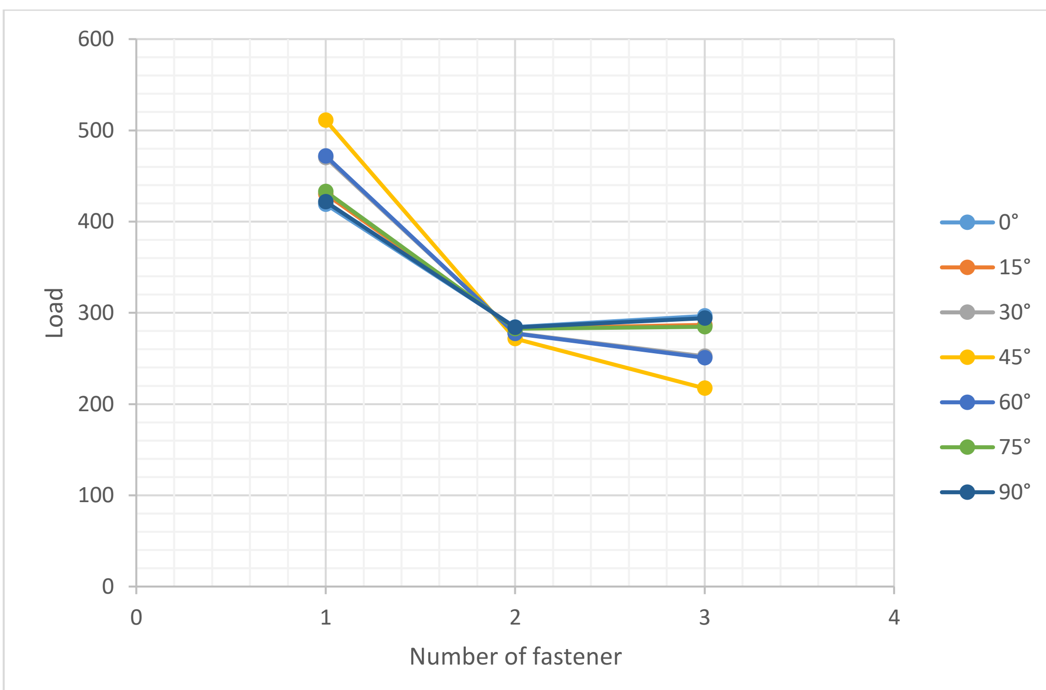

Fig 4.11 for three fasteners

5.

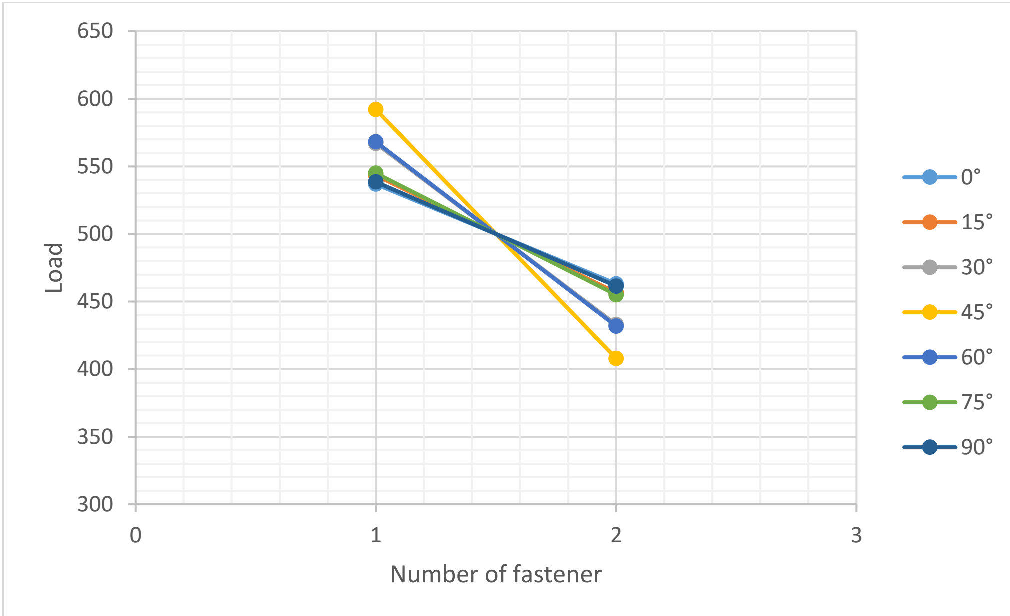

Fig 4.12 for two fasteners

Having analyzed the charts, we can see how the loading pattern changes, depending on, how are the layers of composite placed. A characteristic tendency is the distribution of the load on the fasteners, even a change in the elastic modulus does not significantly change it. The most loaded in all cases are 1st bolts, the general distribution pattern has a stripped parabolic shape.

4.2.2 The dependence of the load distribution depending on the angle of inclination for tape:

1.

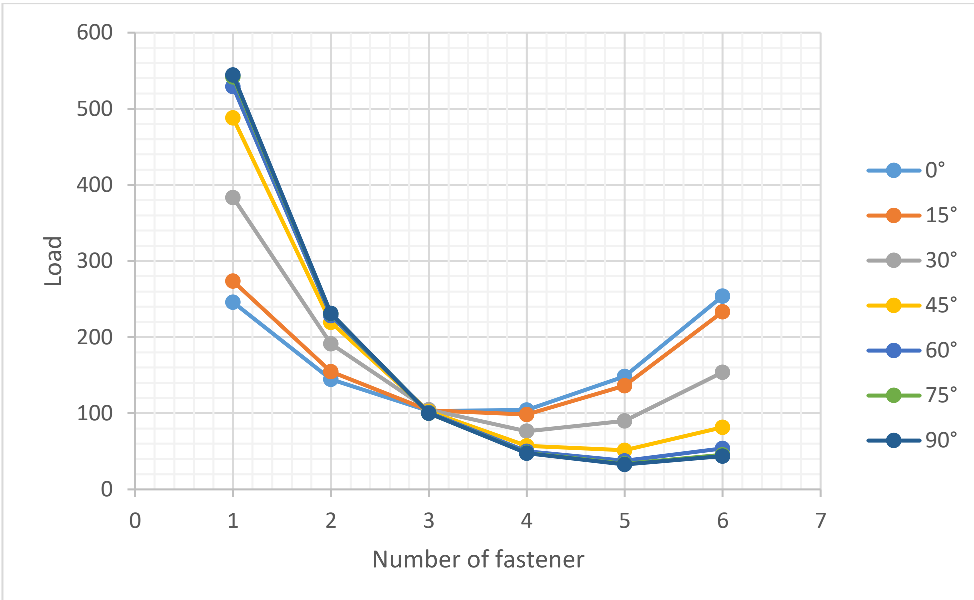

Fig 4.13 for six fasteners

2.

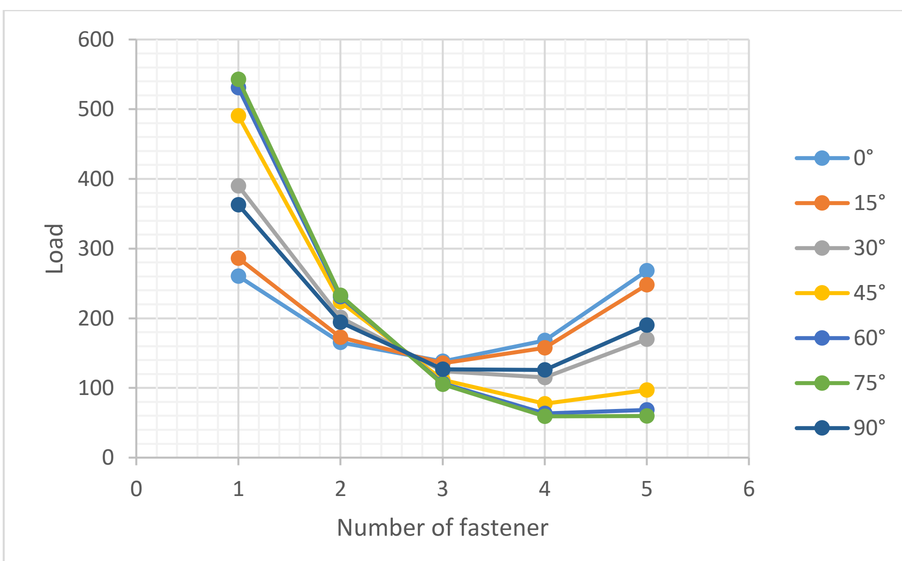

Fig 4.14 for five fasteners

3.

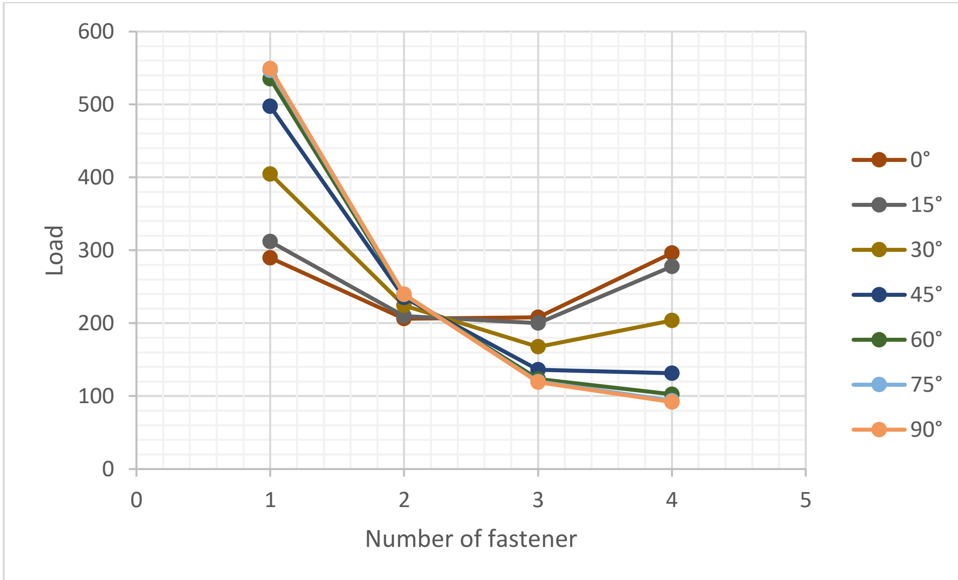

Fig 4.15 for four fasteners

4.

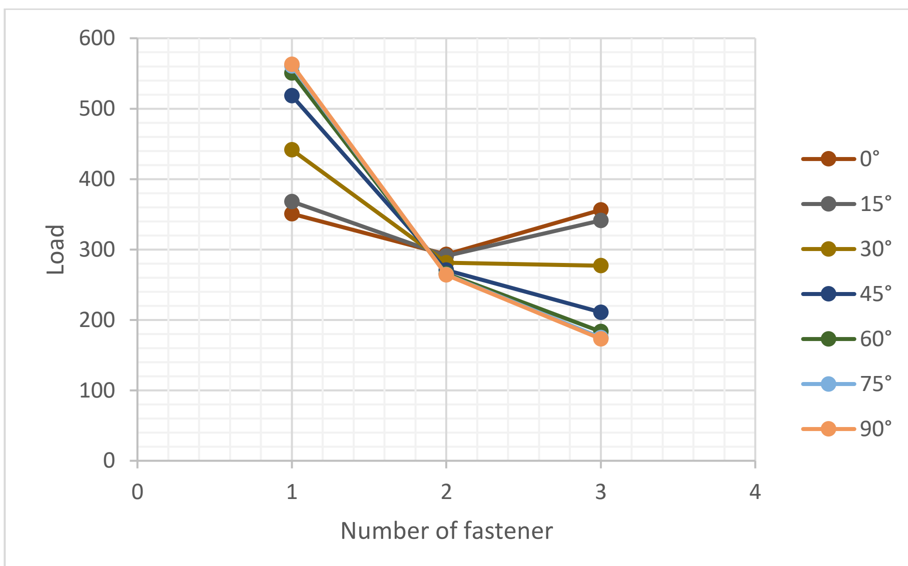

Fig 4.16 for three fasteners

5.

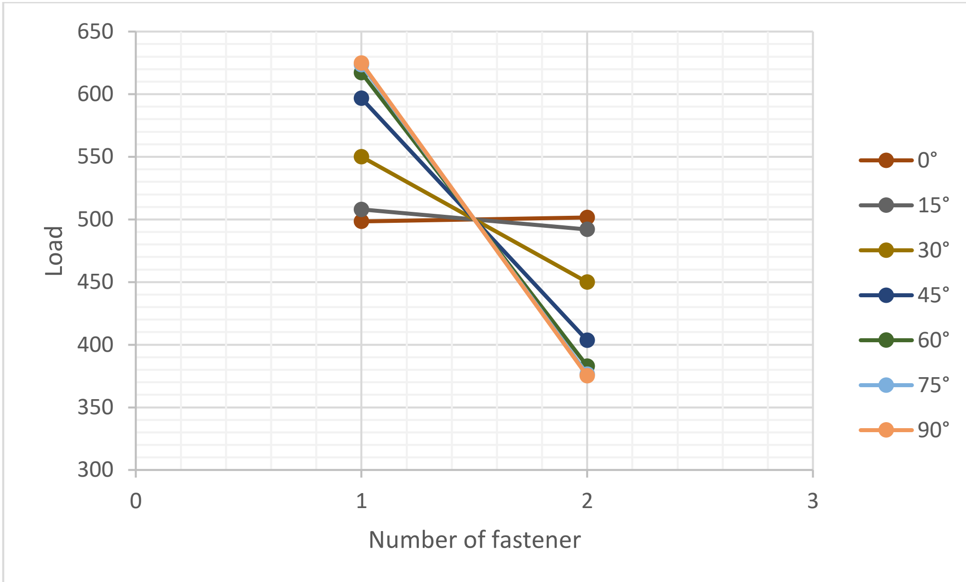

Fig 4.17 for two fasteners

Unlike Fabric, Tape is significantly changes distribution type depending on the rotation angle. When positioned below 0°, all bolts carry almost the same load, but when the fiber is under 90, the 1st bolt carries about 60° percent of the total load.

Having analyzed the data, the load distribution depending on the location of the fibers. It can be concluded that the most appropriate would be to use type under 15°. Because plates in this case carry a load in one direction, but at the same time putting all materials under 0° will be technically not correct. A location at ± 15 degrees helps to avoid this problem and gives the most beneficial result.

It is also worth noting that currently laying composite layers at angles is widespread 0 °; 45 °; 90 °. Therefore, the use of styling at 15 degrees can also be considered an innovation.

4.3 Influence of geometrical characteristics of fasteners on load distribution

We will make the selection of optimal thickness values for each number of fasteners

Table 4.6 Uniform load distribution due to thickness variation

		1	2	3	4	5	6
6	Load distribution, %	16.6	16.7	16.7	16.6	16.9	16.5
	t_s, in	0.073	0.12	0.113	0.065	0.034	0.017
	t_p, in	0.23	0.23	0.23	0.23	0.23	0.23
5	Load distribution,%	20.0	19.8	20.3	20.0	19.9	
	t_s, in	0.075	0.157	0.18	0.08	0.036	
	t_p, in	0.18	0.18	0.18	0.18	0.18	
4	Load distribution, %	25.2	24.9	24.9	24.9		
	t_s, in	0.08	0.175	0.159	0.07		
	t_p, in	0.2	0.2	0.2	0.2		
3	Load distribution, %	33.4	33.3	33.3			
	t_s, in	0.1	0.165	0.1			
	t_p, in	0.2	0.2	0.2			
2	Load distribution, %	50	50				
	t_s, in	0.135	0.15				
	t_p, in	0.2	0.2				

As you can see from table 4.6, limiting ourselves only to a change in thickness, you can get a design that will be difficult to manufacture.

5. Development of a rational design of a highly loaded metal-composite joint

In the previous sections, various methods for calculating fasteners were considered, of which one was selected that gives the most reliable results. The optimum angle of laying of the composite and its type were also selected. All these data are the basis for the development of the desired compound.

Table 5.1 Improved high-load joint parameters

		1	2	3	4	5	6
6	Load distribution, %	16.9	16.4	16.8	16.0	16.6	17.2
	t_s, in	0.09	0.14	0.2	0.14	0.09	0.06
	t_p, in	0.22	0.22	0.22	0.22	0.22	0.22
	D, in	0.3125	0.375	0.375	0.3125	0.25	0.1875
5	Load distribution,%	19.89	19.97	20.05	20.05	20.05	
	t_s, in	0.11	0.19	0.186	0.14	0.08	
	t_p, in	0.2	0.2	0.2	0.2	0.2	
	D, in	0.25	0.3125	0.375	0.3125	0.25	
4	Load distribution, %	25.1	24.9	25.2	24.8		
	t_s, in	0.14	0.15	0.14	0.13		
	t_p, in	0.2	0.2	0.2	0.2		
	D, in	0.1875	0.3125	0.375	0.25		
3	Load distribution, %	33.0	33.7	33.2			
	t_s, in	0.12	0.18	0.16			
	t_p, in	0.2	0.2	0.2			
	D, in	0.3125	0.375	0.3125			

6. Development of a startup project

The startup project in this work is precisely the calculation method, which allows you to develop any required metal- composite joint. Based on the necessary space for its location, the required dimensions of the fasteners (if we add this to an existing structure), depending on the transferred load, select the type and orientation of the composite layers.

This dissertation is, in its essence, a unique template, as does not require additional investments, and based on empirically derived formulas.

The financial component of this template depends only on the ability to sell ready-made solutions, problems encountered by the customer, and the search for customers.

Therefore, a one-time assessment and sale of the template is not rational.

Conclusion

1. Reviewed existing composite metal joint methods.
2. Examined the existing methods for calculating the fasteners flexibility.
3. We calculated the elastic characteristics, Fiber and type for different angles of laying the layers of the composite.
4. We analyzed the influence of such characteristics as: method and angle of laying composite material; geometric details (thickness, diameter of bolts).
5. Developed the most optimal compound in terms of minimum weight.
6. Evaluated the financial component of this project.

References

1. P. Molitor, V. Barron, T. Young **Surface treatment of titanium for adhesive bonding to polymer composites: a review**
Int. J. Adhes. Adhes., 21 (2001), pp. 129-136, 10.1016/S0143-7496(00)00044-0

2. Z. Dawei, Z. Qi, F. Xiaoguang, Z. Shengdun**Review on joining process of carbon fiber-reinforced polymer and metal: methods and joining process**
Rare Metal Mater. Eng., 47 (2018), pp. 3686-3696, 10.1016/S1875-5372(19)30018-9

3. Tierney, J. J., Gillespie Jr. J. W., and Bourban P. E., Comprehensive Composite Materials, volume 2 (2000) pages 1029-1047

4. Stokes Vijay K., Polymer Engineering and Science, volume 29, No. 19, (1989) pages 1310 – 1324

5. Vicík J., Laŝova V., Kosnar M., Janda P. and DvořăK J., Advanced Engineering, volume 4, issue 4 (2010), 2ISSN 1846-5900

6. Moroni F., A. Pirondi, F. Kleiner, International Journal of Adhesion & Adhesives, volume 30 (2010) pages 367–379

7. Kweon Jin-Hwe, Jae-Woo Jung, Tae-Hwan Kim, Jin-Ho Choi and Dong-Hyun Kim, Composite Structures, volume 75, Issues 1 - 4 (2006) pages 192 – 198

8. Camanho P. P., Tavares C. M. L., De Oliveira R., Marques A. T., Ferreira A. J. M., Composites: volume 36, part B (2005) pages 372–383

9. Canyurt O. E., Meran C. and Uslu M., International Journal of Adhesion and Adhesives, volume 30, Issue 5 (2010) pages 281-287

10. Kolesnikkov B., Herbeck L. and Fink A., Composite Structures, volume 83 (2008) pages 368 -380

11. Janardhana M. N., Brown K. C., Jones R. and Paul J., Composite Structures, volume 5, issue 1(1986) pages 1-14

12. Ucsnik S., Scheerer M. , Zaremba S. and Pahr D.H. , Composites Part A: Applied Science and Manufacturing, volume 41, issue 3 (2010) pages 369 – 374

13. Lee Young-Hwan, Do-Wan Lim, Jin-Ho Choi, Jin-Hwe Kweon and Myung-Keun Yoon, Composite Structures, volume 92, issue 12, (2010) pages 2916-2926

14. Chalmers B., Principles of Solidification, Wiley, New York, 1964, pages 158-250

Chan W.S and Vedhagiri S., Journal of Composite Materials, Volume 35, issue 12 (2001) pages 1045 – 1061

15. Hart-Smith L. J., Journal of Aircraft, volume 22, issue 11 (1985) pages 993 – 1000

16. Nelson, W.D., Bunin, B. L., and Hart-Smith, L. J., *Critical Joints in Large Composite Aircraft Structure*. NASA CR 3710. 1983, National Aeronautics and Space Administration: Washington, DC.

17. Lee, J.J., *Design and Analysis of Multirow Highly Loaded Bolt Joints in Composite Wing Structures*, MS Thesis, *Mechanical Engineering*. 2000, California State University, Long Beach: Long Beach, CA.

18. C. Nordin. Bult flexibilitet for drag- och skjuvbelastade skruvforband i KAP. Report FKHK-1-82.045, Saab-Scania, 1982.

19. J. Brandt. Formler for berakning av bultflexibilitet. Preliminar utgava. Report FKH R 3303,Saab-Scania, 1982.

20. W. Barrois. Stresses and displacements due to load transfer by fasteners in structural assemblies. Engineering Fracture Mechanics, 10(1):115{176, 1978

21. Web site

https://www.britannica.com/technology/composite-material

22. Collings, T.A., Experimentally Determined Strength of Mechanically Fastened Joints, in Joining Fibre-Reinforced Plastics, F.L. Matthews, Editor. 1987, Elsevier Applied Science: London, England

23. M. B. Tate and S. J. Rosenfeld. Preliminary investigation on loads carried by individual bolts in bolted joints. Technical Report TN-1051, National Advisory Committee for Aeronautics, 1946.

24. L. Jarfall. Shear loaded fastener installations. Report KH R-3360, Saab-Scania, 1983.

25. H. Huth. Experimental determination of fastener flexibilities. Report LBF-Bericht 4980, Fraunhofer-Institut fur Betriebsfestigkeit, Darmstadt, 1983.

26. Michael C.Y. Niu Composite Airframe COMPOSITE Structures

27. NASA Contactor Report 3710, Critical Joints in Large Composite Aircraft Structure, N87-10973